THE POLAR CAPS

Syun-Ichi AKASOFU

Geophysical Institute, University of Alaska, Fairbanks, Alaska 99775-0800, U.S.A.

Abtsract: In the past we have somewhat slighted upper atmospheric phenomena in the area bounded approximately by the auroral oval because our main interests have traditionally been concentrated on understanding magnetospheric substorms along the auroral oval; substorms are due primarily to the southward component of the interplanetary magnetic field (IMF). However, it has recently become clear that a great variety of fascinating phenomena take place in this highest latitude region of the earth when the IMF has an appreciable northward component. The importance of those phenomena in understanding basic magnetospheric processes is emphasized. Systematic observational programs specifically designed to study those phenomena in the Antarctic region could make significant contributions to upper atmospheric physics and magnetospheric physics.

1. Introduction

The term 'polar cap' has long been used rather loosely in the past (MURPHREE *et al.*, 1982). Perhaps the most common definition of it is the region bounded by the average or statistical auroral oval. As a result, the polar cap has also been considered as a dark and uninteresting region surrounded by the bright auroral oval along which all interesting magnetospheric and ionospheric processes take place. Only as the exception, the so-called 'polar cap arcs' appear from time to time across the area surrounded by the oval. However, such a view of the polar cap has been radically changed during the last few years.

When the north-south component B_z of the interplanetary magnetic field (IMF) has an appreciable southward component, the auroral oval is larger than the average size and brighter, indicating that an auroral substorm is often in progress. The region surrounded by the active auroral oval appears very dark, and there is no prominent feature which can be observed optically. Figure 1 shows an example of auroral images over the Antarctic region, taken from the Dynamics Explorer (FRANK, private communication, 1984). However, drastic changes begin to take place as the IMF B_z component begins to turn northward. As the IMF B_z component remains positive for an extended period (say, >6 hrs), this highest latitude region of the earth becomes the stage of a variety of fascinating phenomena which are most vital in understanding the solar wind-magnetosphere interaction.

We have long slighted auroral phenomena in this highest latitude region of the earth because our main interests have traditionally been concentrated in understanding magnetospheric substorms which are due primarily to the southward component of IMF B_z. Actually, it has been our recent finding that auroral phenomena in this highest region during periods of the IMF $B_z>0$ are at least as complicated and

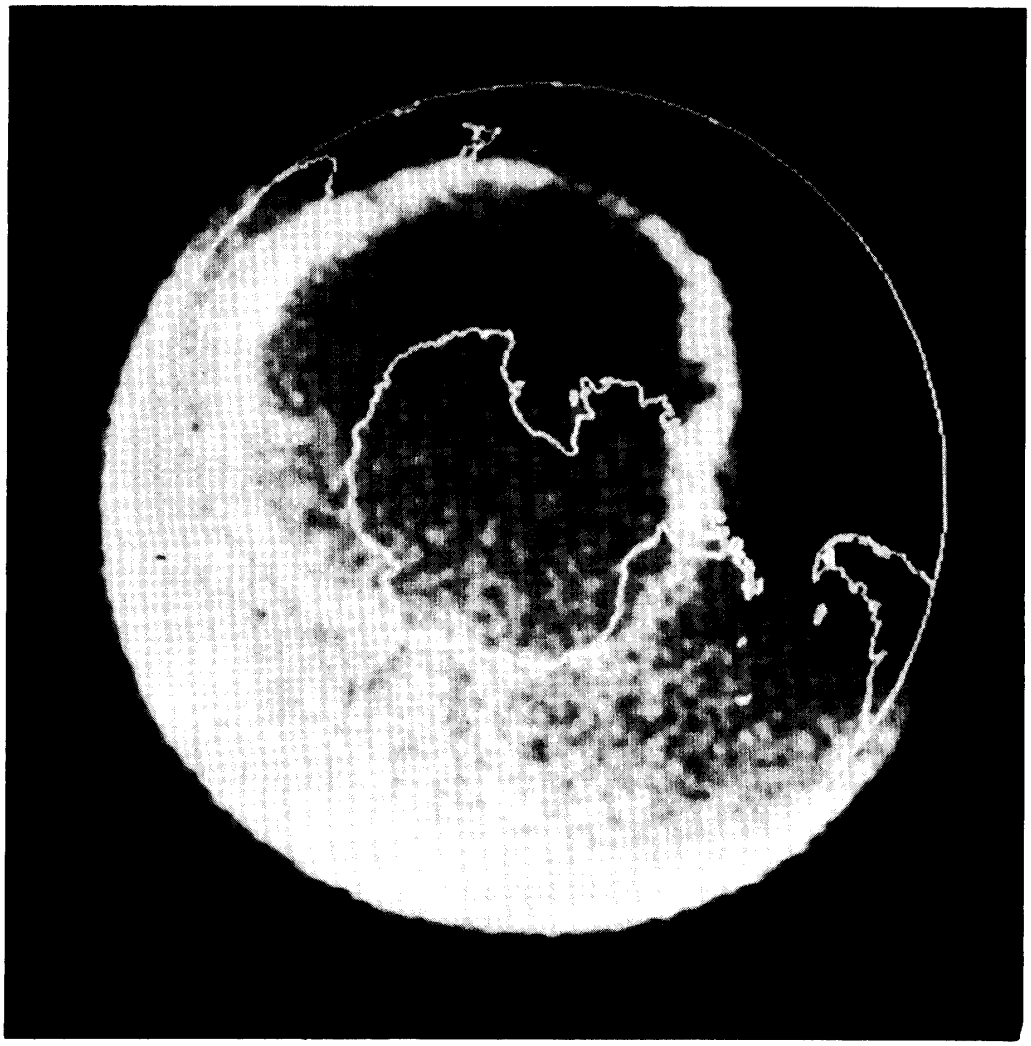

Fig. 1. Auroral oval image in the southern hemisphere taken from Dynamics Explorer at 0859 UT on January 10, 1983 (Courtesy of L. A. FRANK, J. D. CRAVEN and R. D. RAIRDEN, University of Iowa).

fascinating as those in the auroral oval during periods of the IMF $B_z<0$. Therefore, our understanding of the solar wind-magnetosphere interaction would be very incomplete without a detailed study of auroral phenomena during the periods of the IMF $B_z>0$. Furthermore, the B_z component is only one of the components of the IMF vector $\boldsymbol{B}$, so that a full understanding of the solar wind-magnetosphere interaction requires a study of effects of the IMF components B_x and B_y as well. That is to say, we have been studying substorms which are only one aspect of the solar wind-magnetosphere interaction (namely, the effects of the IMF $B_z<0$). However, we must study effects of the IMF $B_z>0$, $B_y\gtrless 0$ and $B_x\gtrless 0$ as well. As we shall see later, the B_z component tends to dominate over the IMF B_x and B_y components in controlling the solar wind-magnetosphere interaction when it has the southward component; this is due to the fact that the earth's dipole moment is approximately directed southward. Therefore, effects of the IMF $B_y\gtrless$ and $B_x\gtrless 0$ can be examined more easily under the condition of the IMF $B_z>0$ than that of the IMF $B_z<0$.

In this paper, we review studies of effects of the IMF $B_z>0$, $B_y \gtrless 0$ and $B_x \gtrless 0$ on various upper atmospheric phenomena. The Antarctic region is the stage for such investigations, as well as the Arctic region. Thus, we shall often refer to Antarctic observations in the paper, hoping that some of the discussions in this paper will be useful in formulating future Antarctic observations. It is important that Antarctic observations are unique and innovative, providing new insights into magnetospheric processes, rather than repeats of Arctic observations. For this purpose, it is important to sort out some of the most critical problems in magnetospheric physics today and devise innovative methods to solve them, taking advantage of a diverse background of Antarctic scientists, a close cooperative nature of the efforts among them, the single landmass, a very high shadow height over the South Pole station around magnetic noon in May, June and July, etc. In this paper, we emphasize particularly those observations in the highest latitude region which throw some light on corresponding changes of the internal structure of the magnetosphere.

2. Definition and Working Definition of the Polar Cap

There is little doubt that there exists a limited area in the highest region of the earth, from which the open field lines originate; here, the open field lines are defined as the geomagnetic field lines which are 'interconnected' or 'reconnected' with IMF lines. During a solar electron event after solar flares, there is an area in which energetic solar electrons impinge almost *uniformly* over the highest region, indicating that the solar electrons have an equal chance of access over a nearly circular area. In Fig. 2, one can see how uniformly these electrons reach over a wide range of latitude as the satellite traversed the highest latitude region approximately along the noon-midnight meridian. Thus, this area is likely to be the open field line region. This is because the best available method to trace the open field lines is to use solar electrons

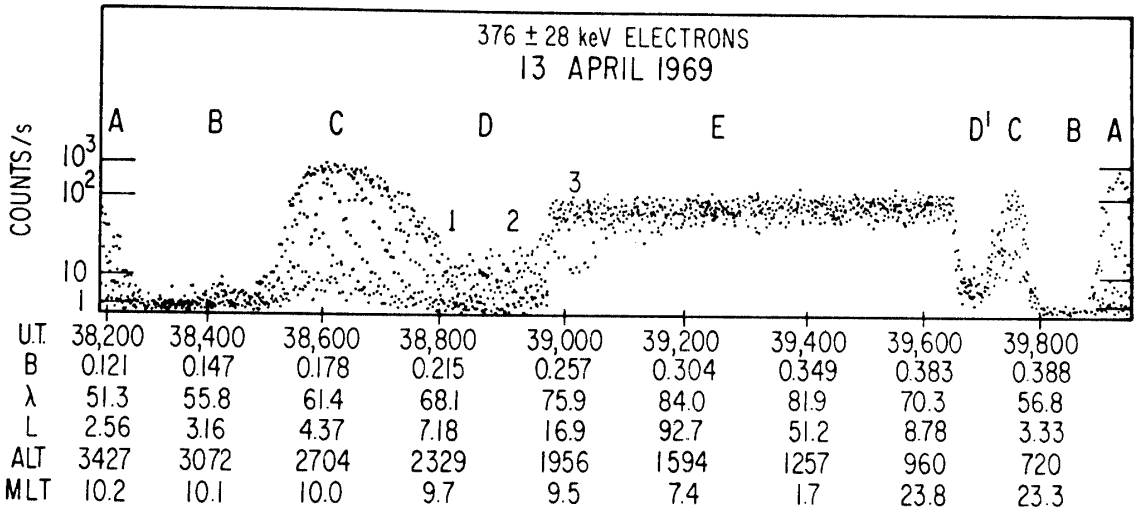

Fig. 2. Observation of electrons of energies of 376±28 keV by a polar orbiting satellite. As the satellite traversed the polar region from the dayside to the nightside, it encountered a high and constant flux of the electrons from about 75° in the dayside to about 65° in the nightside (VAMPOLA, 1971).

of energies of the order of a few hundred kilovolts. Such electrons tend to follow the original field lines as they started. Electrons of less energies will be susceptible to the $\boldsymbol{E}\times\boldsymbol{B}$ drift and protons of even much less energies would not follow the same field line. Further, this area has a geometry which is similar to the area bounded by the auroral oval. In Fig. 2, the uniform flux was encountered at about the latitude of the cusp ($\sim 76°$) and ended at about the latitude of the midnight oval ($\sim 65°$).

Perhaps, the most meaningful definition of the polar cap is the open field line region. The boundary of the open field line region thus defined is one of the most important natural coordinates in studying magnetospheric phenomena. As mentioned earlier, however, the term 'polar cap' has only loosely been defined in the past, and it is generally considered that it is the region bounded by the average or statistical auroral oval. Many workers use both the region bounded by the average or instantaneous oval and the open field line region synonymously. However, this loose definition of the term 'polar cap' encounters various problems. For example, do the so-called 'polar cap arcs' appear in the open field line region? That is to say, are the field lines which guide electrons to the so-called 'polar cap arcs' open or closed? Clarification of this question alone will eliminate a number of possible mechanisms of the formation of 'polar cap arcs'.

Further, this most meaningful definition of the polar cap, namely the open field line region, encounters practical difficulties, namely how one can delineate the boundary of the open field line region. Perhaps it is a reasonable working definition that the open field line region is bounded by the instantaneous oval when the IMF B_z component is negative and the expansive phase of a substorm is in progress. However, identifying the open field line region based on the above working definition becomes increasingly difficult and obscure when the IMF B_z component turns northward and the substorm begins to recover. Suddenly, auroral activity inside the region bounded by the pre-existing oval increases (*cf.* LASSEN and DANIELSON, 1978). Often, a large number of auroral arcs and diffuse glow appear in this area (*cf.* MURPHREE *et al.*, 1982). Thus, it becomes very difficult to define the open field line region on the basis of the distribution of auroras. These auroral phenomena in the highest latitude region during the time when the IMF B_z component becomes positive must be manifestations of large-scale changes of the structure of the magnetosphere, so that it is important to examine simultaneously both polar cap phenomena and magnetospheric phenomena. Eventually, both phenomena should be explained mutually consistently.

3. The IMF and Magnetospheric Models

It is instructive to examine effects of the three components of the IMF vectors on the basis of a simple modeling method. We construct first a model of the magnetosphere without the presence of the IMF, using the standard procedure, namely by having an image dipole and the tail current system. The IMF is then superposed by a linear superposition in a vacuum situation. We test the qualitative validity of this method by determining the geometry of the open field line region for a set of the observed values of the IMF three components, B_x, B_y and B_z and then comparing the geometry of the open field line region thus determined with the geometry of the

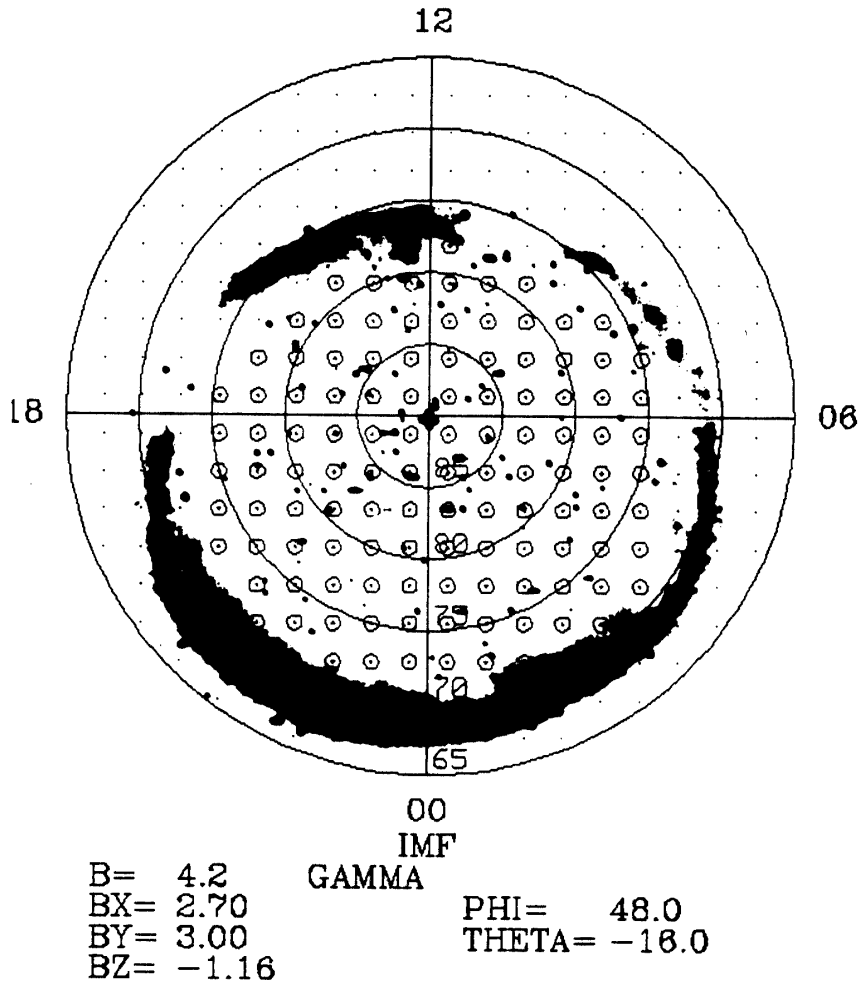

*Fig. 3. Test of a magnetospheric model. An observed IMF is superposed, and the open field line region is determined. The 'simultaneously' observed auroral oval is shown together with the computed open field line region (*MURPHREE *et al., 1984).*

oval about one hour after the IMF observation. An example of such tests is shown in Fig. 3 (MURPHREE *et al.*, 1984). In the figure, a dot indicates the foot of a closed field line. That is to say, a field line originating at the location of a dot reaches the conjugate point in the southern hemisphere after crossing the equatorial plane, while a circled dot indicates the foot of an open field line. The field line originating at the location of a circled dot is connected to the IMF field line across the magnetopause. One can see that the open field line region is fairly accurately bounded by the poleward boundary of the observed oval. It is quite obvious that the above test can provide only a qualitative validity of our modeling and the fair agreement of the boundary of the open field line region and the poleward boundary of the oval may be fortuitous, particularly because we are using a simple (vacuum) superposition method. Nevertheless, such a modeling method may provide some guidance in interpreting complicated upper atmospheric phenomena in the highest latitude region, particularly when the IMF B_z is positive. We shall see in the following that this is indeed the case.

For this purpose, we assume an IMF vector of magnitude of 5 nT. Then, we

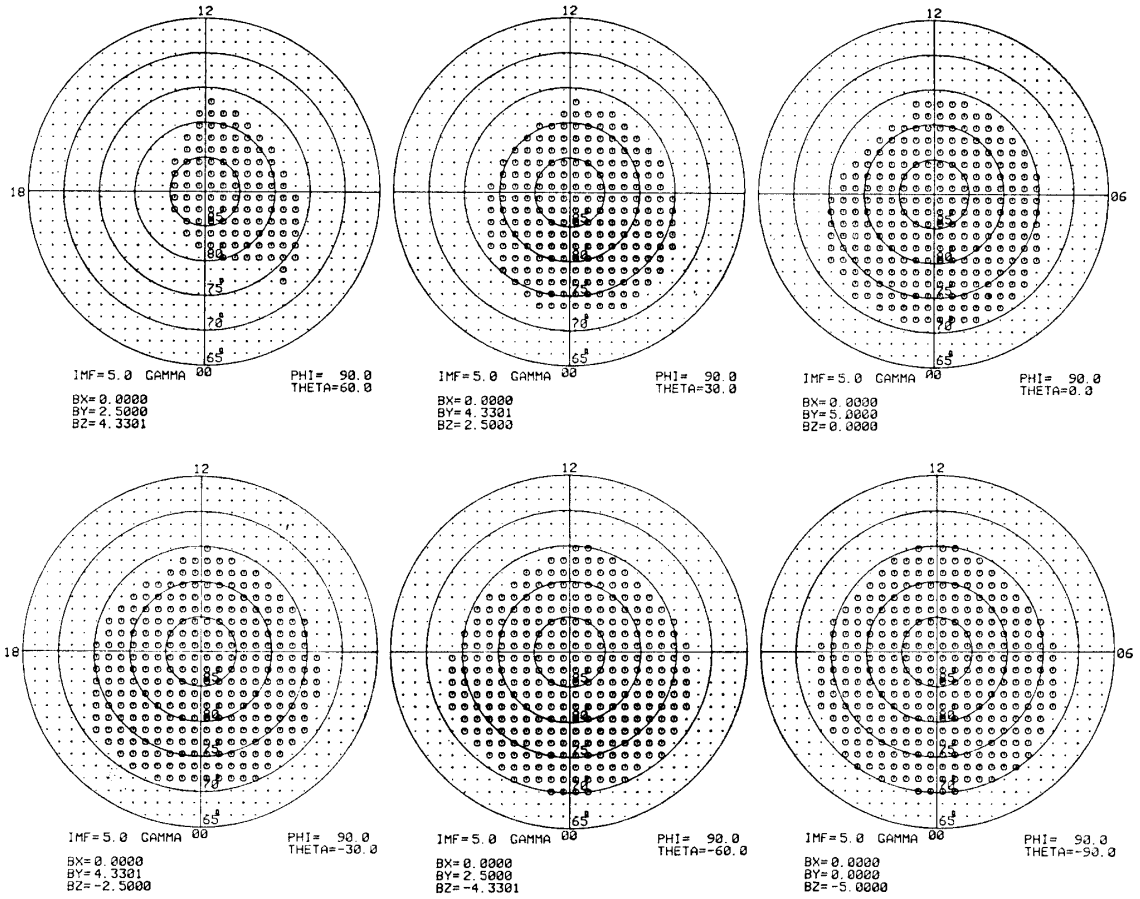

Fig. 4. Changes of the geometry of the open field line region as the IMF vector of $\mathbf{B}=5$ *nT in the y-z plane rotates (AKASOFU and ROEDERER, 1984).*

examine changes of the geometry of the open field line region for two situations: (i) the IMF vector lies and rotates in the *y-z* plane, and (ii) the IMF vector lies and rotates in the *x-z* plane.

(a) Rotation in the *y-z* plane

The lower right diagram in Fig. 4 shows the geometry of the open field line region when the IMF vector is directed southward ($B_x=0$, $B_y=0$, $B_z=-5$ nT); for details see AKASOFU and COVEY (1980) and AKASOFU and ROEDERER (1984). The boundary of the open field line region thus obtained is similar to the poleward boundary of the auroral oval which is a little larger than the average one. Effects of the rotation of the IMF vector can clearly be seen by examining in turn the lower middle, lower left, upper right, upper middle and upper left diagrams. One of the interesting features revealed by such a study is that the geometry of the open field line region changes only a little with the rotation of the vector so long as the B_z component is negative. In fact, those changes are, perhaps, difficult to identify by observations. The asymmetry of the open field line region with respect to the noon-midnight meridian becomes obvious only when the B_z component becomes zero or positive. For IMF $B_x=0$, $B_y=2.5$ nT, $B_z=+4.3$ nT (the latitude angle $\theta=60°$), the main part of the open field line region is confined in the morning sector. Since the IMF B_z component can-

not cause the asymmetry with respect to the noon-midnight meridian, the asymmetry must be caused by the IMF B_y component. It should be noted that the simultaneous open field line region in the southern hemisphere is the mirror image of the northern one, so that it is mainly confined in the evening sector for the same IMF three component values. It should also be noted that when the B_y component is negative ($B_z=0$, $B_y=-2.5$ nT, $B_z=+4.3$ nT), the whole situation is reversed; the open field line region in the northern hemisphere is mainly confined in the evening sector, while the southern one is confined in the morning sector.

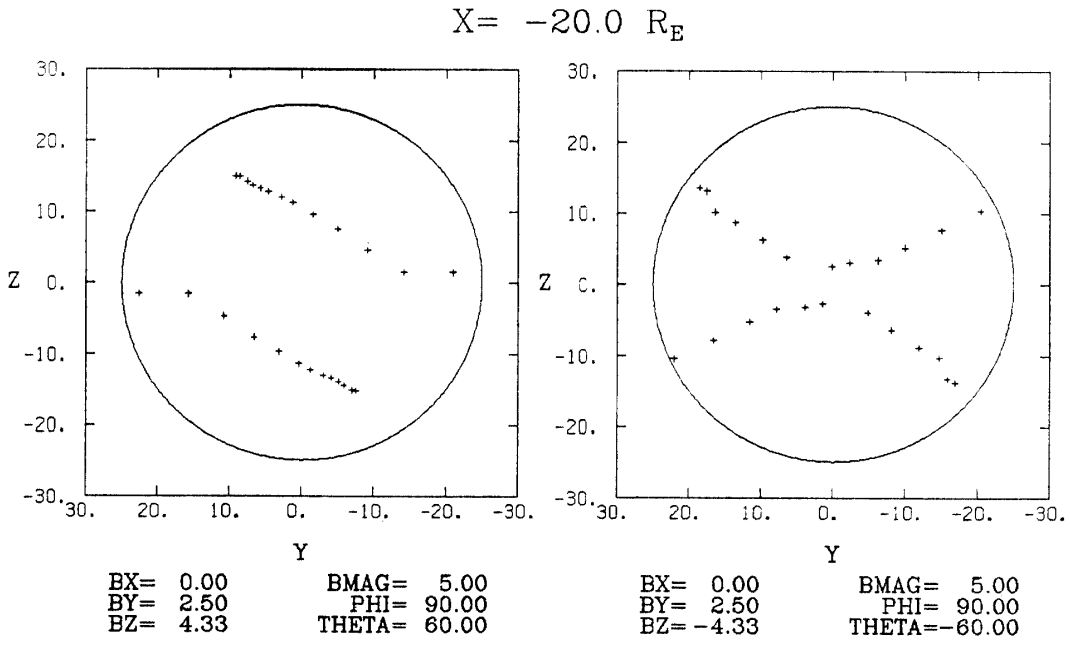

Fig. 5. The cross-section of the plasma sheet (views toward the earth) at $X=-20R_E$ for the two IMF conditions (i) $B_x=0$, $B_y=2.50$ nT, $B_z=+4.33$ nT, and (ii) $B_x=0$, $B_y=2.50$ nT, $B_z=-4.33$ nT (AKASOFU and ROEDERER, 1984).

The corresponding distribution of the plasma sheet becomes asymmetric with respect to the noon-midnight meridian and the equatorial plane, causing a tilting of the plasma sheet. Figure 5 shows the computed cross-section of the plasma sheet at $X=-20$ R_E for the conditions in the upper left and lower middle of Fig. 4. Again, when the IMF B_z component is negative, the IMF B_y effect is small; the tilting of the plasma sheet can be seen clearly when the IMF B_z component is positive.

(b) Rotation in the x-z plane

Here, we rotate the IMF vector (of magnitute 5 nT) by 360° in the x-z plane. In the upper left diagram of Fig. 6a, the IMF is pointed northward ($B_x=0$, $B_y=0$, $B_z=+5$ nT). Then, as the vector is rotated toward the sun ($B_x>0$) the open field line region has a circular shape and becomes larger; the lower left diagram shows the situation when the vector is pointing directly toward the sun. Then, as the vector is rotated further and thus has the southward component (IMF $B_z<0$), the open field line region is very much like the area bounded by the average auroral oval. As the vector is further rotated, it points away from the sun ($B_x<0$) and has the southward

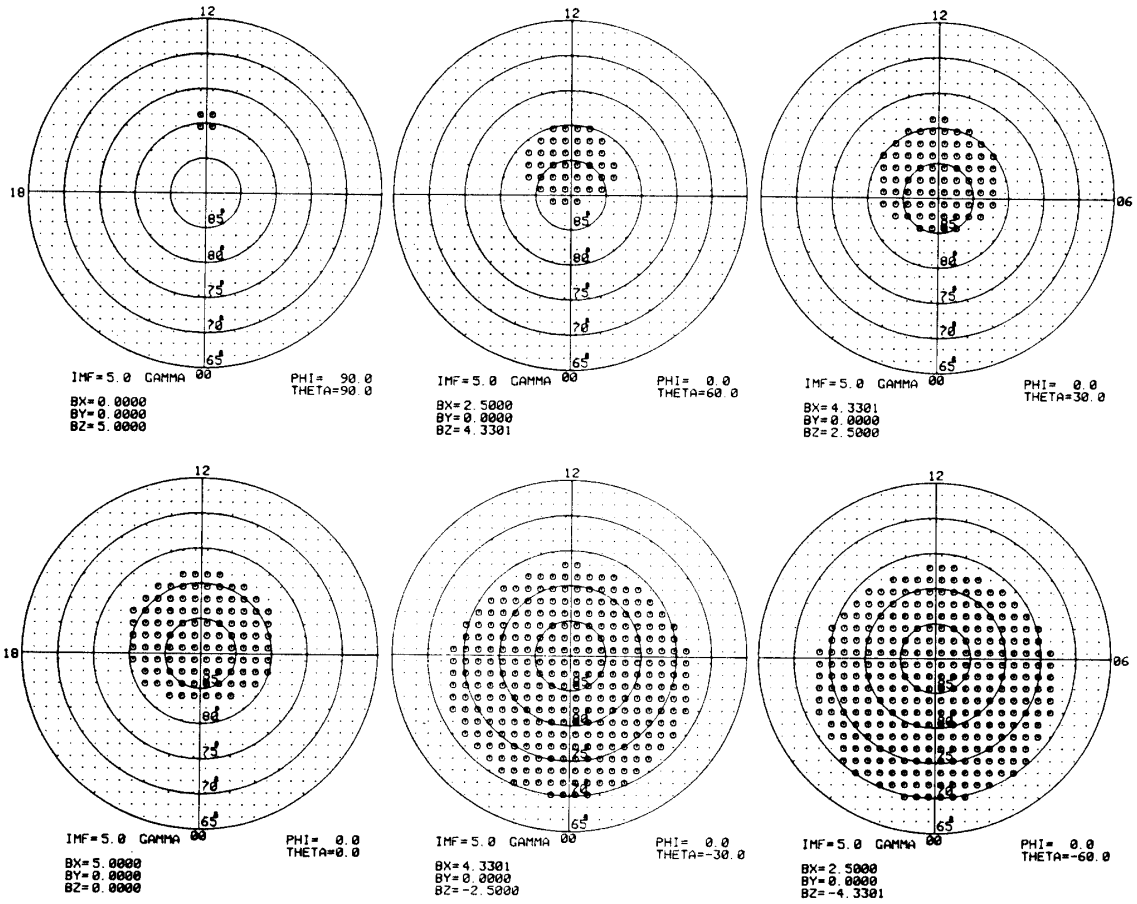

Figs. 6a and 6b. Changes of the geometry of the open field line region as the IMF vector of $\boldsymbol{B}=5$ *nT is rotated in the x-z plane (AKASOFU and ROEDERER, 1984).*

component (the two lower diagrams in Fig. 6b). The open field line region is still similar to the area bounded by the average oval. The upper right diagram shows the situation when the vector points directly away from the sun. As the vector is further rotated and the B_z component becomes positive (the upper left and middle diagrams), the open field line region has a crescent shape.

Therefore, once again, when the IMF B_z component has a negative value, the open field line region has the geometry which is close to that bounded by the average oval. However, the open field line region has a considerably different geometry, when the IMF B_z component has a positive value. Note also when the IMF has ($B_x=-2.5$ nT, $B_y=0$, $B_z=+4.33$ nT), the northern open field line region has a crescent shape, while the geometry of the simultaneous southern region is the same as that for ($B_x=2.5$ nT, $B_y=0$, $B_z=+4.33$ nT).

In the following several sections, we shall examine effects of the IMF three components for various polar upper atmospheric phenomena.

4. Entry of Solar Energetic Electrons

As mentioned earlier, solar energetic electrons are, in general, perhaps the best

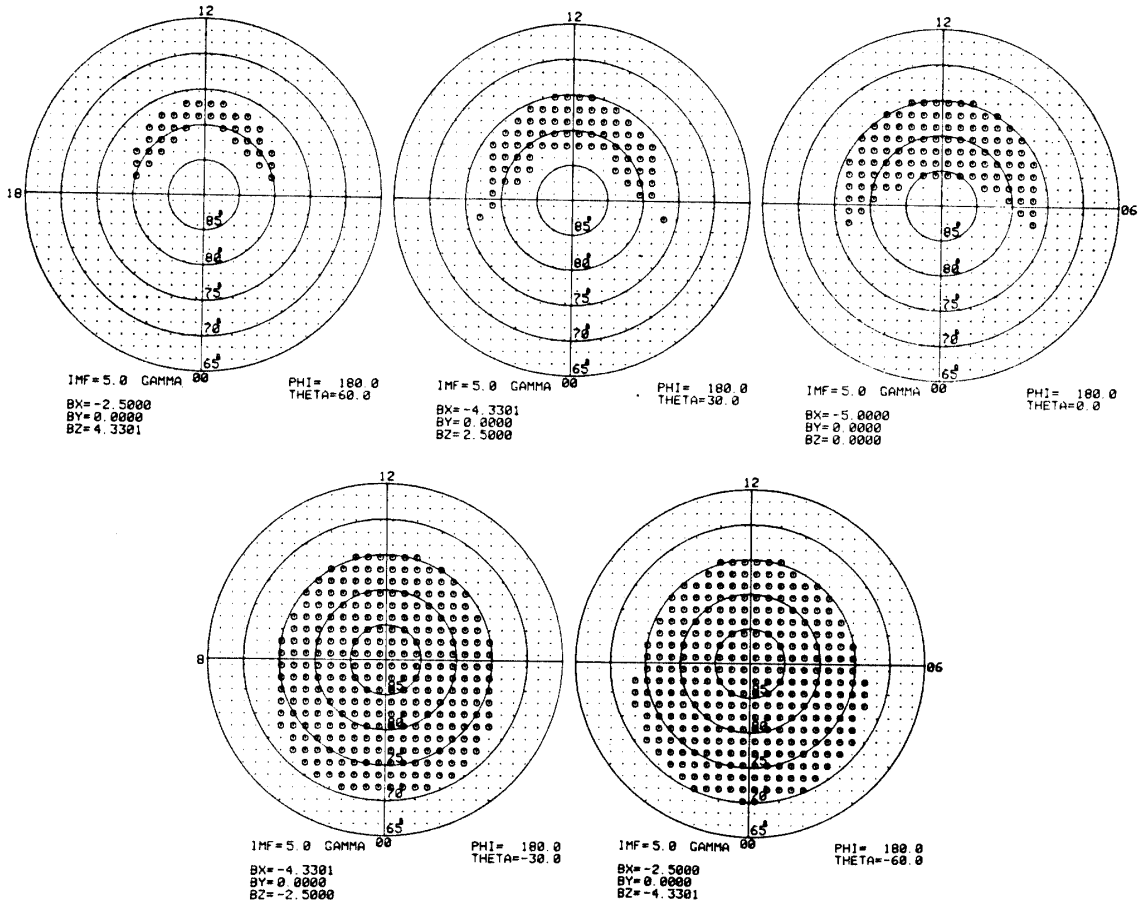

Fig. 6b.

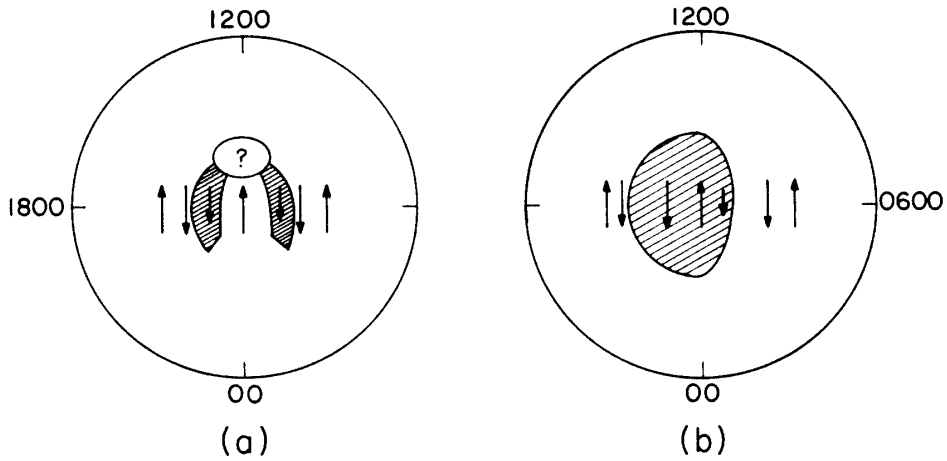

Fig. 7. Area of the entry of solar energetic electrons for two IMF conditions (a) $B_x = -20$ nT, $B_y = -5$ nT, $B_z = +30$ nT, and (b) $B_x = 4.3$ nT, $B_y = -0.7$ nT, $B_z = +9.2$ nT (McDiarmid et al., 1980).

tracer of magnetic field lines. McDiarmid *et al.* (1980) examined the area of entry of solar energetic electrons for various IMF orientations. Figure 7 shows schematically the entry area for (a) IMF $B_x = -20$ nT, $B_y = -5$ nT, $B_z = +30$ nT, and (b) IMF

B_x=4.3 nT, B_y=−0.7 nT, B_z=+9.2 nT. One can see qualitative similarities between the upper left open field line region in Figs. 6b and 7a and between the upper left one in Fig. 4 (by reversing the sign of the B_y component) and Fig. 7b. In fact, such a close agreement with a very crude modeling method is remarkable (AKASOFU *et al.*, 1981).

One of the problems in determining the open field line region by the entry of solar energetic electrons is that their flux is high enough to be used only after a major solar flare, so that this method will not be available at all times. Nevertheless, it is important to extend the work made by MCDIARMID *et al.* (1980) in studying the geometry of the open field line region for various IMF orientations. As we shall see later, other

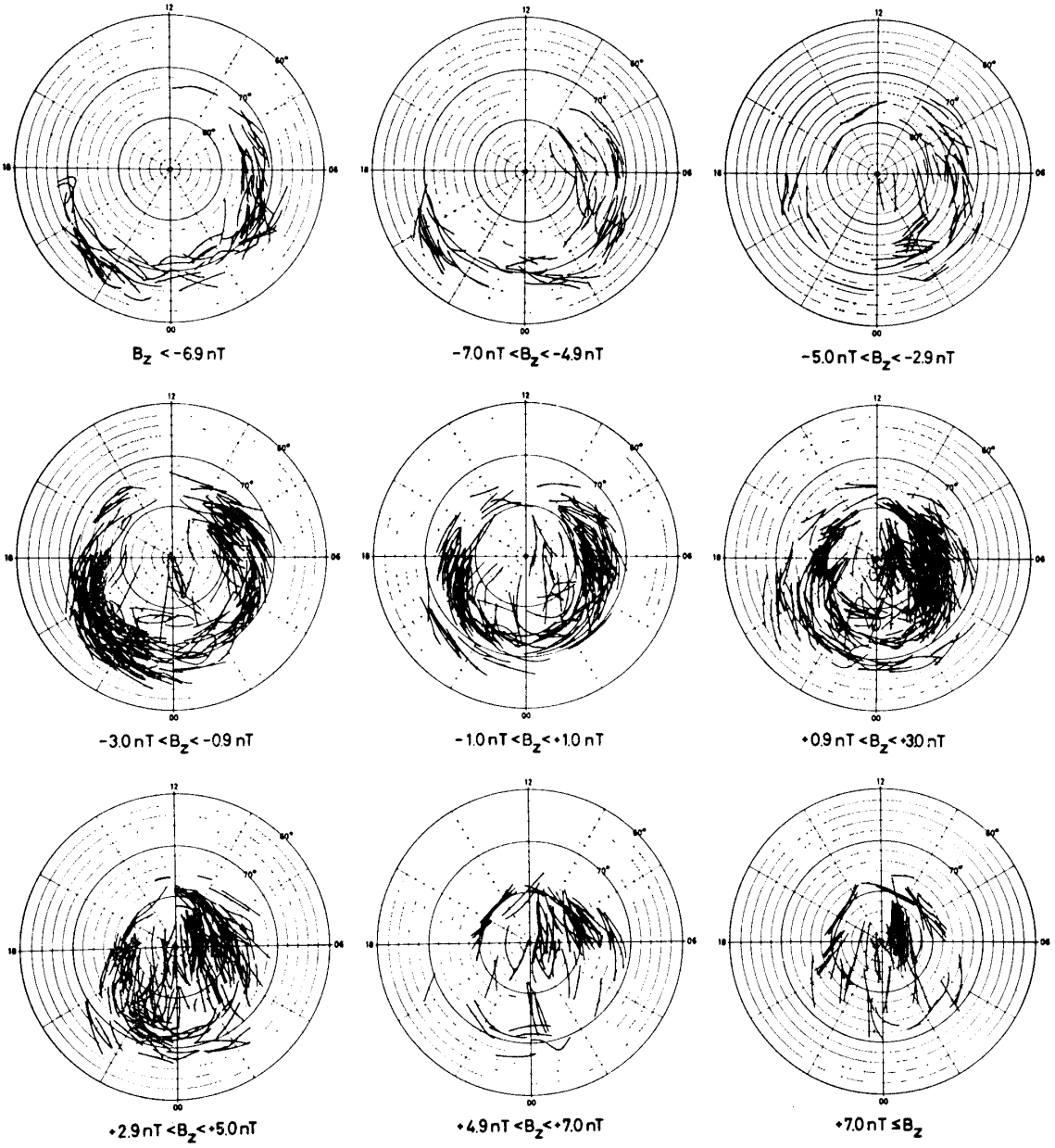

Fig. 8. Distribution of auroral arcs for different values of the IMF B_z component (LASSEN and DANIELSEN, 1978).

methods of inferring the geometry of the open region have great uncertainties.

5. Aurora

5.1. *Statistical studies*

Effects of the IMF B_z component on the distribution of the aurora were most systematically studied by LASSEN and DANIELSEN (1978). Their figure is reproduced here in Fig. 8. One can see clearly that when the IMF B_z component has a large negative value (−6.9 nT), (i) the auroral oval is large and (ii) there is no auroral arc inside the area bounded by the enlarged oval. As the other extreme situation of a large positive B_z value (> +7.0 nT), there is no clear indication of auroral arcs along an oval-shaped belt. Instead, the highest latitude region is covered by arcs which align

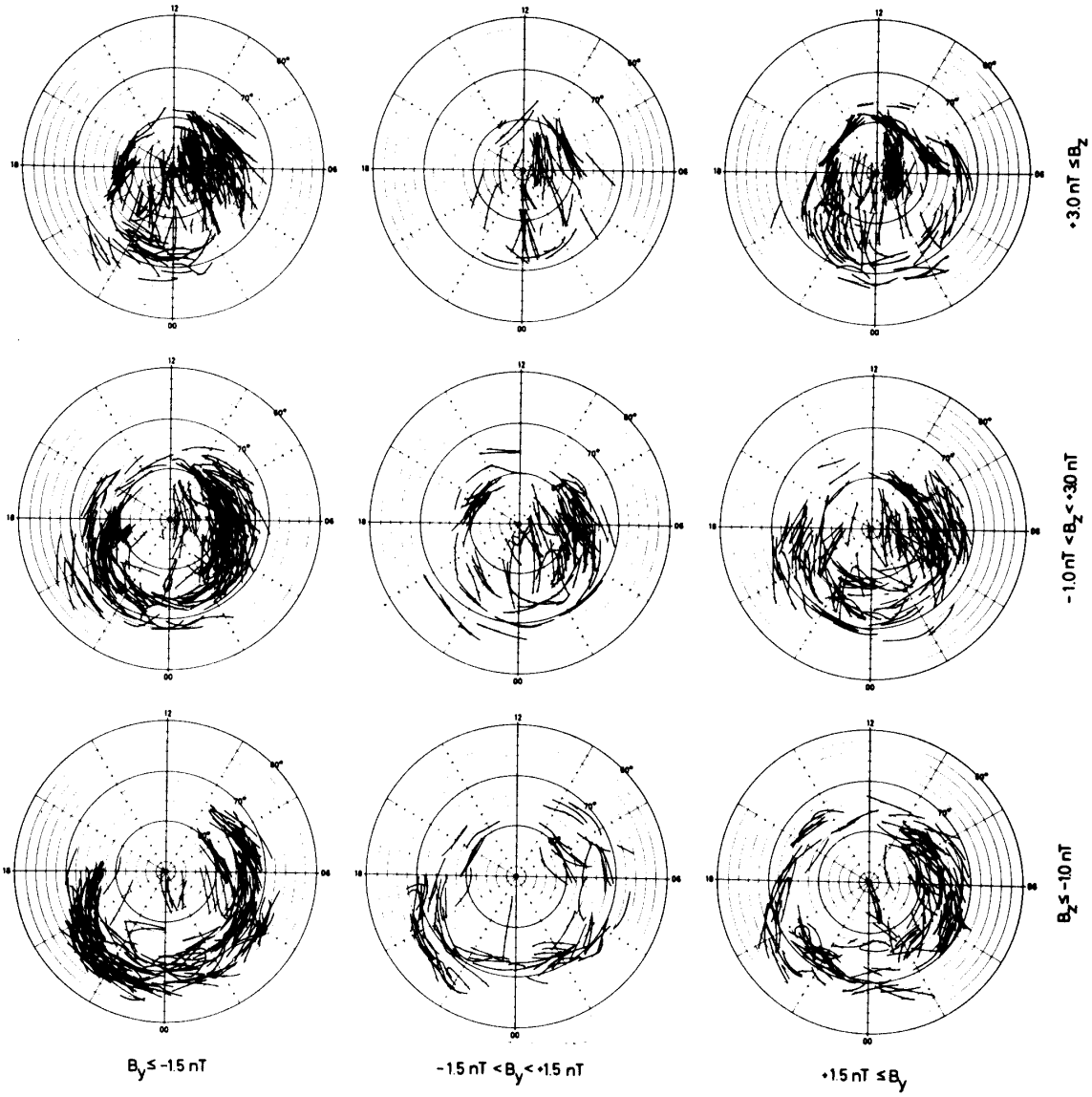

Fig. 9. Distribution of auroral arcs for different combinations of the IMF B_y and B_z component values (LASSEN, 1979).

approximately along the sun-earth line. For other values of the B_z component, the auroral distribution varies systematically between the above two extreme situations.

It is not difficult to understand why the auroral oval and the area bounded by the oval are large for a negative value of IMF B_z. The power ε of the solar wind-magnetosphere dynamo is given by

$$\varepsilon = VB^2\sin^4(\theta/2)l_0^2 = \left(\frac{B_{\tan}}{4\pi}\right)V\Phi ,$$

where V and $B_{\tan}$ are the solar wind speed and the tangential component of the magnetic field just inside the magnetopause, respectively, and Φ denotes the open flux (AKASOFU and AHN, 1980). Therefore, the power ε and the open flux Φ are proportional.

Effects of the IMF B_y component during the period of positive values of the B_z component were also examined by LASSEN (1979). His results are reproduced as Fig. 9. As one can see, effects of the B_y component are not necessarily very clearly brought out in his study. However, he suggested that for $B_y>0$ there is an area of auroral absence in the morning sector, while for $B_y<0$ it is located in the evening sector.

5.2. Individual events

Since the above statistical results are not necessarily obvious in individual events, we examine here a very fortunate event, during which both B_y and B_z components had very large values for many hours. Such events occurred on January 10–11 and 15, 1983. In Figs. 10a and 10b, we see a series of the nightside half of the auroral oval,

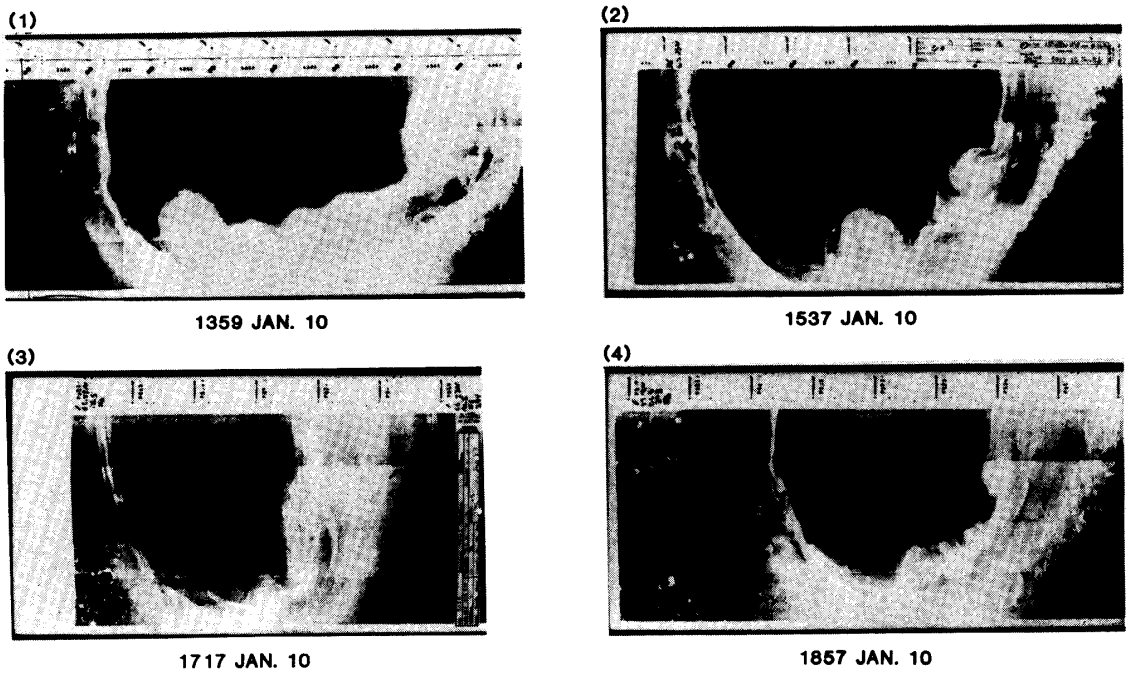

Fig. 10a.

Fig. 10a and 10b. DMSP-F6 images of the nightside half on January 10–11, 1983 (AKASOFU and TSURUTANI, 1984).

obtained by the DMSP-F6 satellite, on January 10 and 11. In the first photograph (1359 UT), the auroral oval was very large, and the auroral activity was high, indicating the typical substorm features; note that the bottom center is approximately the midnight sector, the upper left and upper right corners are approximately the 18 and 06 MLT meridians, respectively. In the second photograph (1537 UT), the oval became smaller and the aurora became less active. However, the major auroral activity is confined in the morning half of the oval, instead of the midnight sector. In the third and fourth photographs, the oval became even smaller (partly due to the geographic effects). Further, the width of the auroral oval in the morning sector became considerably larger than that in the evening sector, making the area bounded by the oval very asymmetric with respect to the noon-midnight meridian; and the center of the area of auroral absence was located in the evening sector. The situation was similar at 1857 UT. The first photograph on January 11 (0653 UT) shows that there occurred a major change after the last photograph (1857 UT on January 10) had been taken. The auroral oval was absent (or became too faint to be registered). On the other hand, a number of auroral arcs occupied approximately the area bounded by the average oval. In the following photograph (1520 UT), those arcs disappeared, and instead there appeared two bright arcs. Further, at 1752 UT, there was a faint glow covering an area which resembles the area bounded by the auroral oval; there were several faint arcs as well.

It is instructive to examine the corresponding IMF data (Fig. 10c); see AKASOFU and TSURUTANI (1984). Initially, the B_z component was negative and had a large magnitude. The B_y component was equally large and negative. The magnitude of

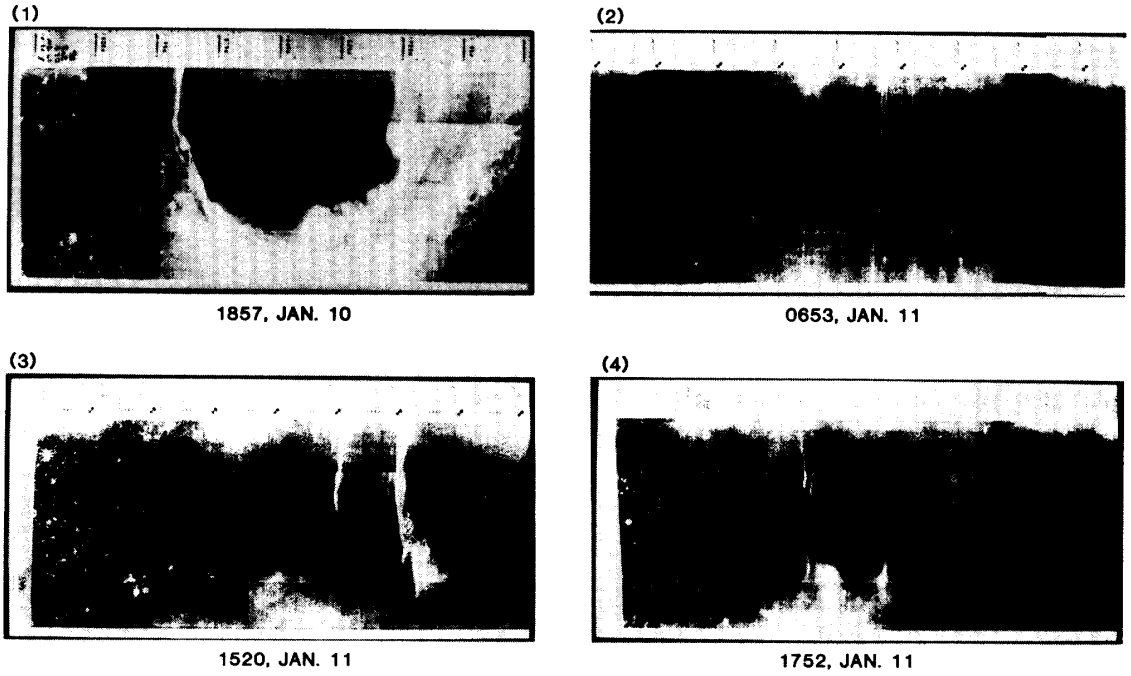

Fig. 10b.

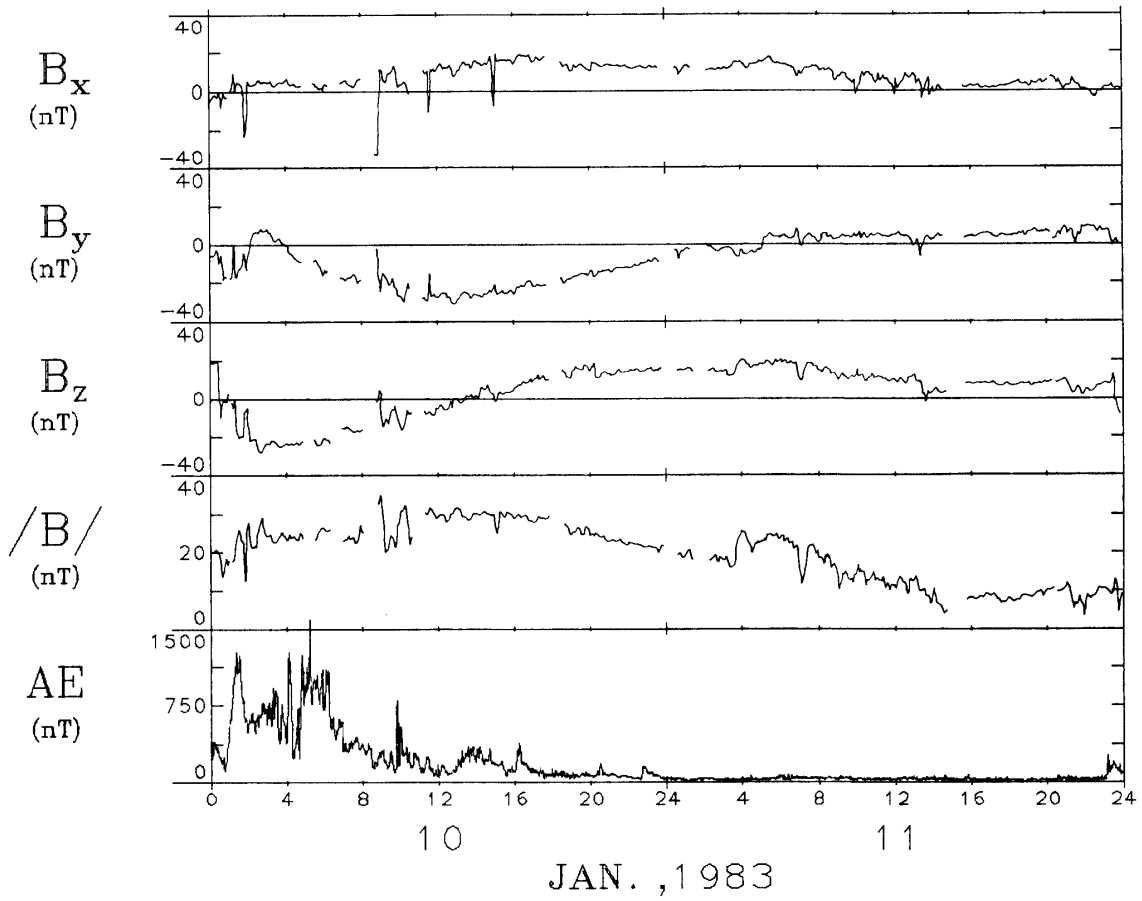

Fig. 10c.

Fig. 10c. IMF B_x, B_y, B_z, B and the AE index on January 10 and 11, 1983, recorded by the ISEE-3 satellite (AKASOFU and TSURUTANI, 1984).

the B_z component became less as the time progressed and became positive at ~14 UT. However, the B_y component remained negative. It changed the sign at ~06 UT and had a small magnitude. Therefore, the B_y (<0) effect became apparent only after the IMF B_z component became positive, and the center of the area of auroral absence was located in the evening sector. Thus, this series of observations are qualitatively consistent with the results of the statistical studies by LASSEN and DANIELSON (1978) and LASSEN (1979). Assuming that the area of auroral absence coincides with the open field line region, the result is consistent with our model study as far as the asymmetry caused by the B_y component is concerned.

After 04 UT on January 11, the B_z component became the dominant component. The appearance of a large number of arcs aligned parallel to the noon-midnight meridian and of the oval-shaped faint glow are one of the most interesting features associated with this large magnitude of the positive B_z component. This particular event is, in fact, under an intensive study by a number of groups at the present time. It is also important that several more individual events of this kind are examined in establishing the auroral morphology during a prolonged period of a large IMF $B_z>0$. At present time, we know little as to how such dramatic changes are related to changes in the magnetotail. In particular, it is of great interest to know whether or not the

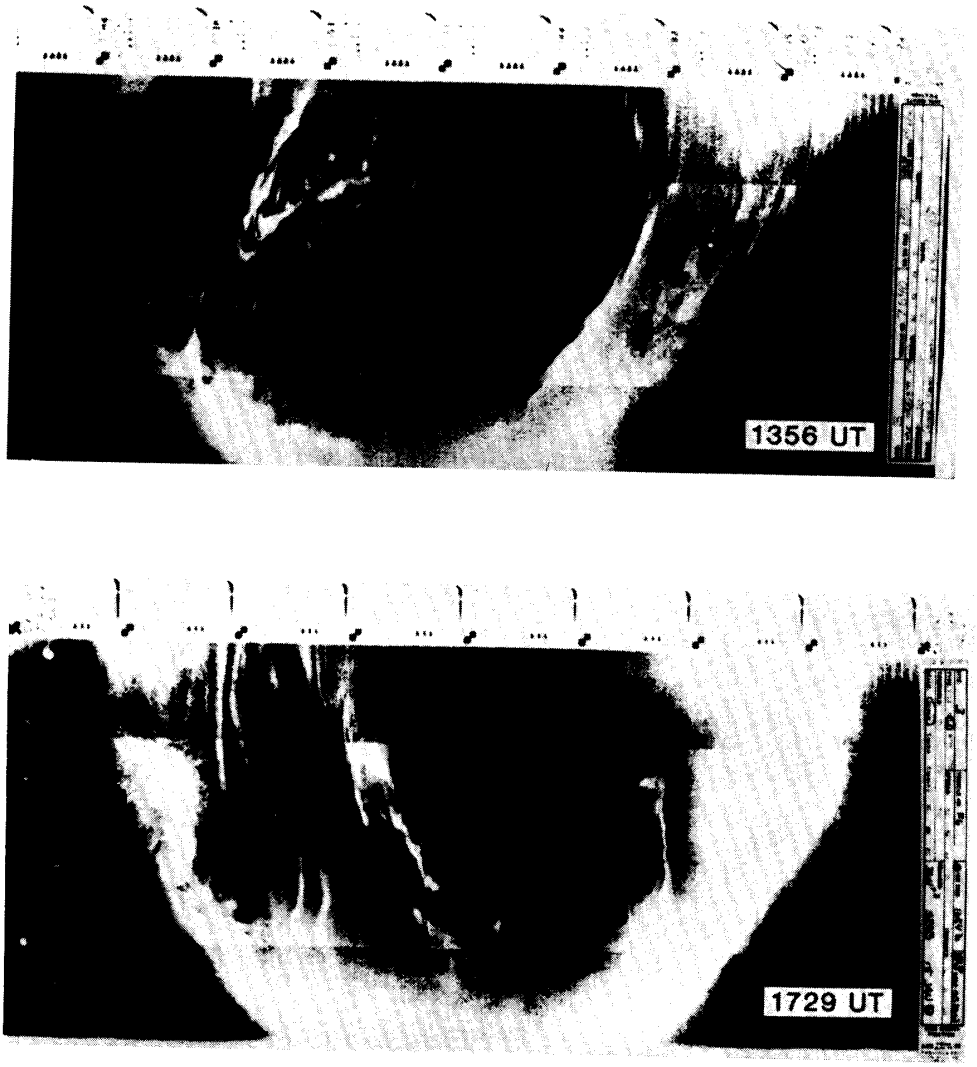

Fig. 11a. DMSP-F6 images of the nightside half on January 15, 1984.

magnetosphere has a closed configuration under such a condition.

Figure 11a shows the auroral distribution during the latter half of January 15, 1983. The IMF B_y and B_z components had large positive values intermittently during this period (Fig. 11b). One can see that the width of the oval in the evening sector is much larger than that in the morning sector. As a result, the center of the area bounded by the oval was located in the morning sector. Therefore, consistent with LASSENS's study and our model study, this tendency can be interpreted as the effect of the B_y component. However, this trend is not necessarily always very obvious.

5.3. Polar cap arcs

It has long been known that there occur auroral arcs in the highest latitude region during the quiet period and that they tend to align parallel to the noon-midnight meridian. It was MAWSON (1925) who documented in detail characteristics of these arcs and was quoted as saying that he could infer the time of a day by observing the

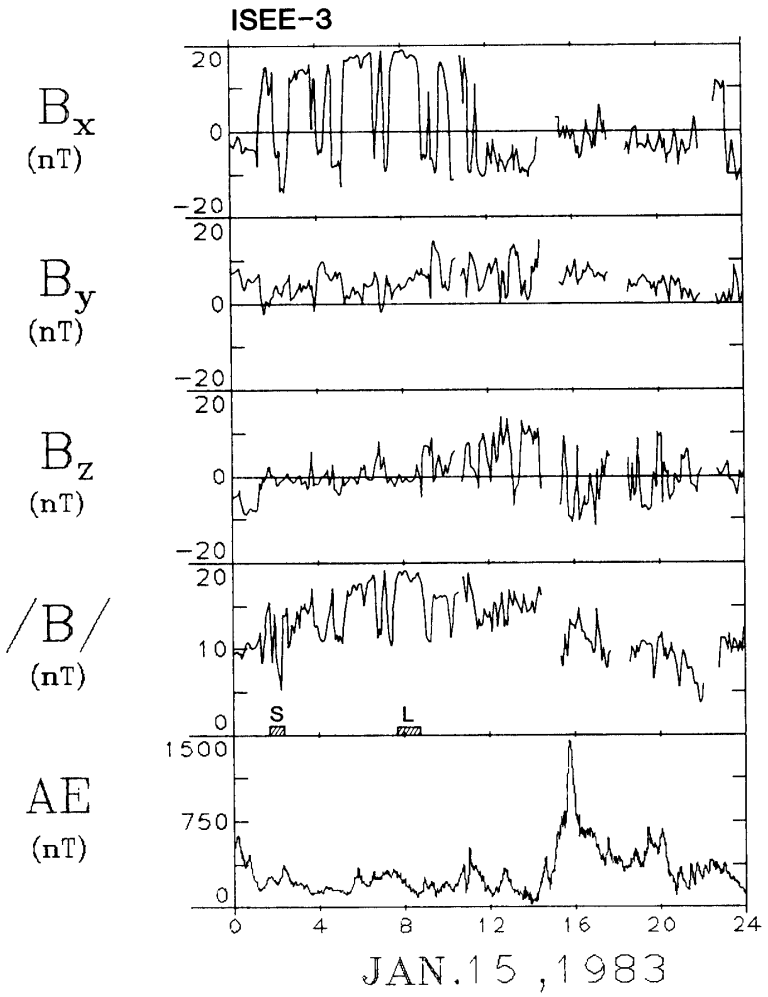

Fig. 11b. IMF B_x, B_y, B_z, B and the AE index on January 15, 1983 (Courtesy of E. SMITH).

orientation of such arcs (since a ground observer will see a complete rotation of the arc orientation during the course of a day as he rotates under sun-aligned arcs once a day). Some of the important characteristics of these arcs are (AKASOFU and ROEDERER, 1983):

1) They tend to align parallel to the noon-midnight meridian (MAWSON, 1925; DENHOLM, 1961; DAVIS, 1962; LASSEN, 1969).

2) Their geometrical structure is identical to discrete arcs along the auroral oval, namely a curtain-like structure.

3) They tend to appear during magnetically quiet periods or during periods when the IMF B_z component is positive (LASSEN, 1969, 1972, 1979; ISMAIL and MENG, 1982; BERKEY *et al.*, 1976; LASSEN and DANIELSON, 1978).

4) They drift in the direction perpendicular to their alignment direction, either dawnward or duskward, with a speed of a few hundred m/s (AKASOFU, 1972).

5) They bend near the midday and midnight parts of the oval and align along oval arcs (AKASOFU, 1972; MENG and AKASOFU, 1976; MURPHREE *et al.*, 1982; ISMAIL and MENG, 1982).

6) Their spectra are characterized by a relatively intense OI 6300 emission

(EATHER and AKASOFU, 1969; ISMAIL *et al.*, 1977). The electron spectra for visible arcs have the so-called "mono-energetic peak" (MENG, 1978; HARDY *et al.*, 1982).

7) They are associated with upward field-aligned currents (SAFLEKOS *et al.*, 1978, 1982).

8) There is a slight indication that they appear more in the morning sector for $B_y<0$ and in the evening sector for $B_y>0$ in the northern polar region (LASSEN, 1979; ISMAIL and MENG, 1982; see also GUSSENHOVEN, 1982).

9) There are upward flowing ionospheric ions above the 'polar cap arcs' (PETERSON and SHELLEY, 1984; YAU *et al.*, 1984).

10) Most recently, FRANK *et al.* (1982a, b) observed the polar cap arcs on a global scale. On one occasion, a polar cap arc was observed continuously for several hours.

Thus, their general characteristics are very similar to those of arcs which appear along the oval, except for the sun-aligned orientation. Therefore, the formation mechanisms for these arcs and oval arcs must be at least very similar and perhaps identical. These arcs have traditionally been called the 'polar cap arcs' and have received much attention during the last two years as spectacular auroral images taken from Dynamics Explorer have become available (FRANK *et al.*, 1982a, b).

Perhaps, the most intriguing question related to the so-called 'polar cap arcs' is the internal structure of the magnetosphere associated with them and how such structural changes are produced by a positive value of the IMF B_z component. It is generally believed that the portion of the auroral oval occupied by discrete auroras (auroral arcs) is connected to the upper (lower) boundary layer of the plasma sheet (namely, BPS) in the northern (southern) hemisphere. Thus, the magnetic field lines permeating the discrete arcs and the boundary layer of the plasma sheet are thought

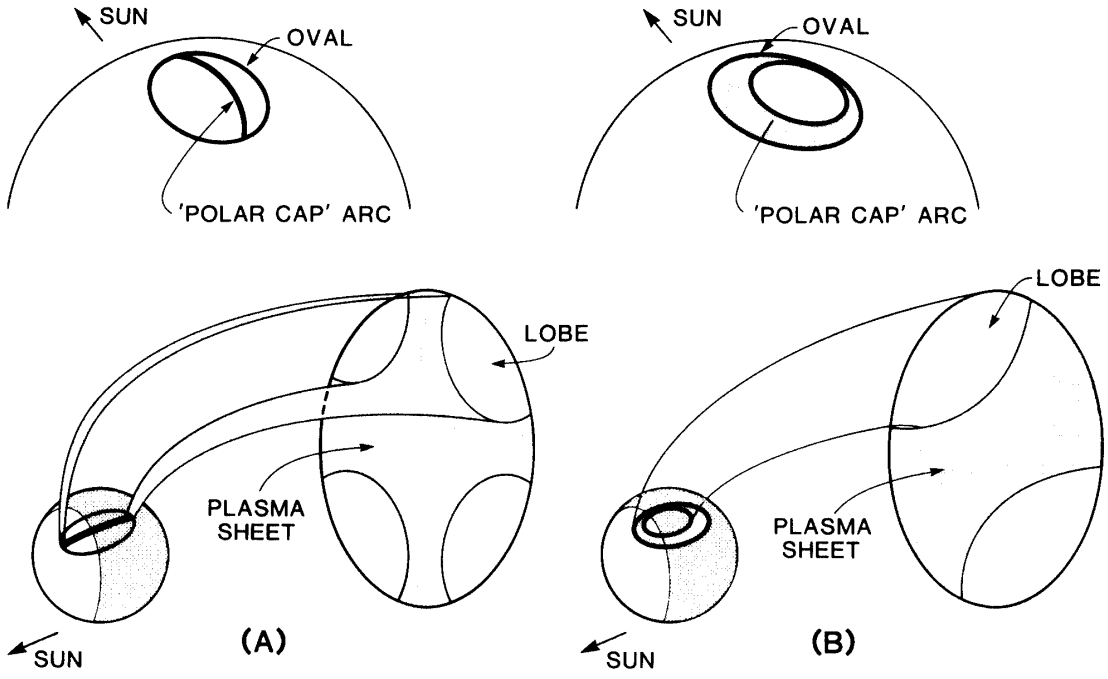

Fig. 12. Two different views on the formation of 'polar cap arcs' and the related magnetospheric structure.

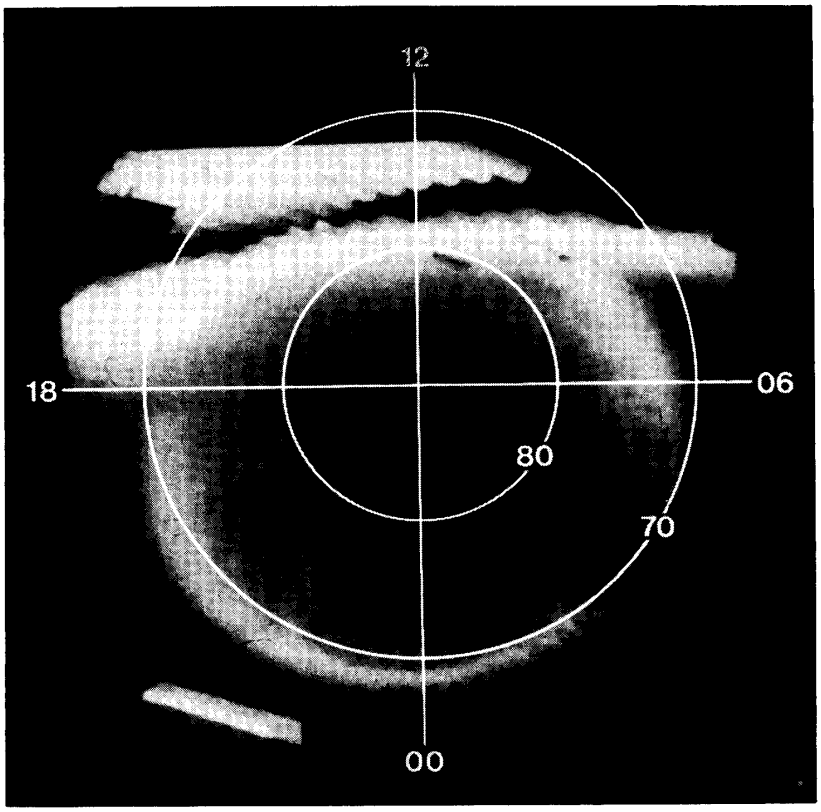

Fig. 13. Example of the 'tear-drop' shape open field line region (MURPHREE et al., 1982).

to be closed. Then, since 'polar cap arcs' and oval (discrete) arcs are very similar, the field lines connected to 'polar cap arcs' may also be closed.

If this would indeed be the case, the plasma sheet may have to develop a structure which bifurcates the high latitude lobe and the open field line region. This situation is schematically illustrated in Fig. 12a. This is certainly an interesting possibility. HUANG *et al.* (1984) showed an interesting plasma observation in the 'lobe' region in the midnight section of the magnetotail, when a 'polar cap arc' was seen by Dynamics Explorer. On the other hand, our modeling study suggests that the open field line region tends to be singly bounded so long as the IMF is uniform around the magnetosphere. In this view, one possibility is that bright auroral arcs form near the boundary of the asymmetric oval caused by the B_y component. Figure 12b shows schematically this situation (MENG, 1981a). Figure 13 shows an example of what one might call the 'tear-drop' shape open field line region (MURPHREE *et al.*, 1982), along which bright arcs are present. As we learned in Section 3, such asymmetry of the open field line region will be accompanied by the tilting of the plasma sheet (Fig. 5). Indeed, the tilting of the plasma sheet similar to that in Fig. 5 has recently observed by the ISEE-3 satellite when the IMF B_y component was large (SIBECK *et al.*, 1985).

Another possibility is that the open field line region is divided into two areas temporarily during the passage of the IMF tangential discontinuities across which the B_y component changes the sign. Figure 14a shows a modeling study of the bifurcation of the open field line region by an IMF discontinuity (AKASOFU *et al.*, 1984). In this situation, some of the magnetospheric field lines are connected to the IMF lines

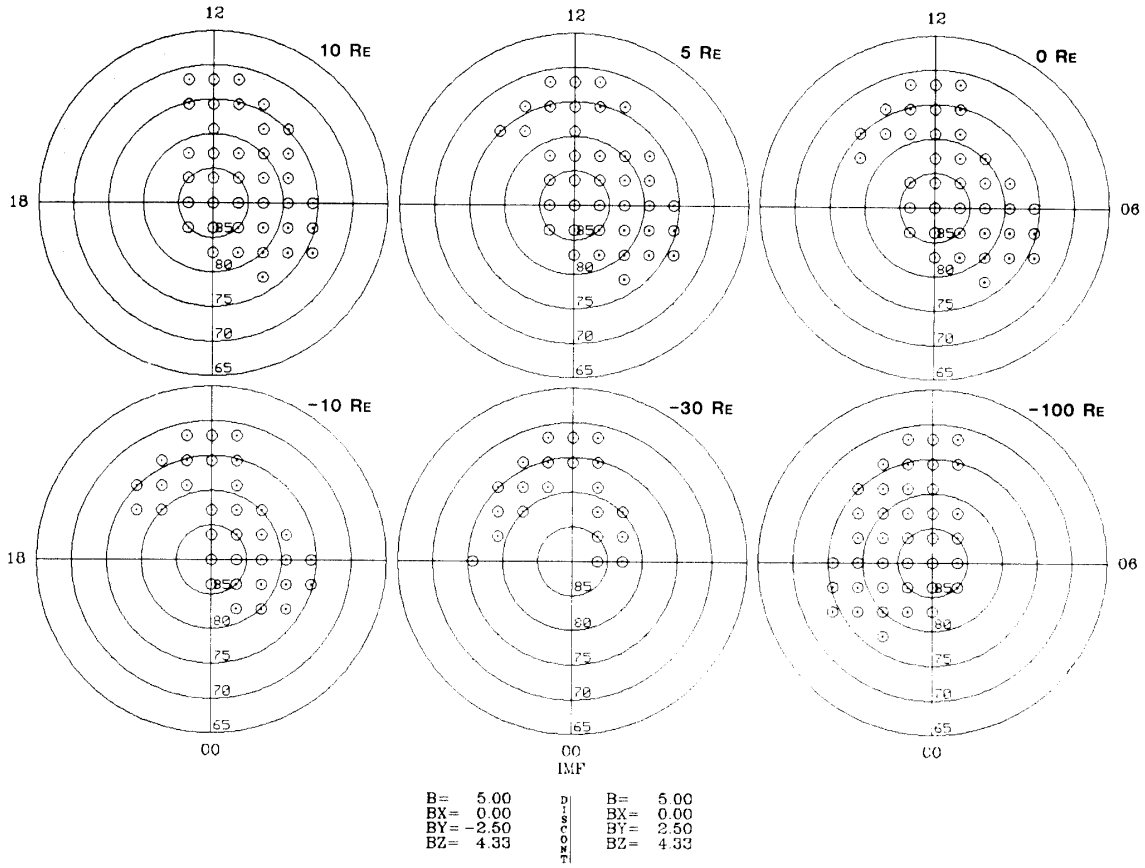

Fig. 14a. Computed bifurcation of the open field line region by and IMF discontinuity (AKASOFU et al., 1984).

in the front side of the discontinuity and the other part to those in the hind side. As the discontinuity (say $B_y<0/B_y>0$) advances from the front of the magnetosphere to the tail, the geometry of the open field line region changes from the type shown in the upper left in Fig. 4 to its mirror image with respect to the noon meridian. In this transit time, the open region may split into two. One example examined by FRANK *et al.* (1985) could be interpreted in this way, because the IMF B_y component changed the sign at the beginning of the event shown in Fig. 14b. Yet, another possibility is that the magnetospheric convective motion in the closed magnetospheric configuration (IMF $B_z>0$) causes the plasma sheet to develop a sheet-like structure perpendicular to it. Figure 14c shows a simulation result obtained by OGINO and WALKER (1984), in which the plasma sheet develops a vertical structure in the midnight sector. In Section 6, a schematic illustration of the convection pattern proposed by KAN and BURKE (1985) is shown. For other theoretical studies of the polar cap arc, see LYONS (1985) and CHIU *et al.* (1985). Systematic auroral observations in the Antarctic region, together with a suitable satellite data set, may be able to tell us which possibility is most likely or unlikely.

5.4. Cusp aurora

AKASOFU (1976) noted that the auroral oval consists of two auroral systems, one centered in the midday sector and the other centered in the midnight sector. This

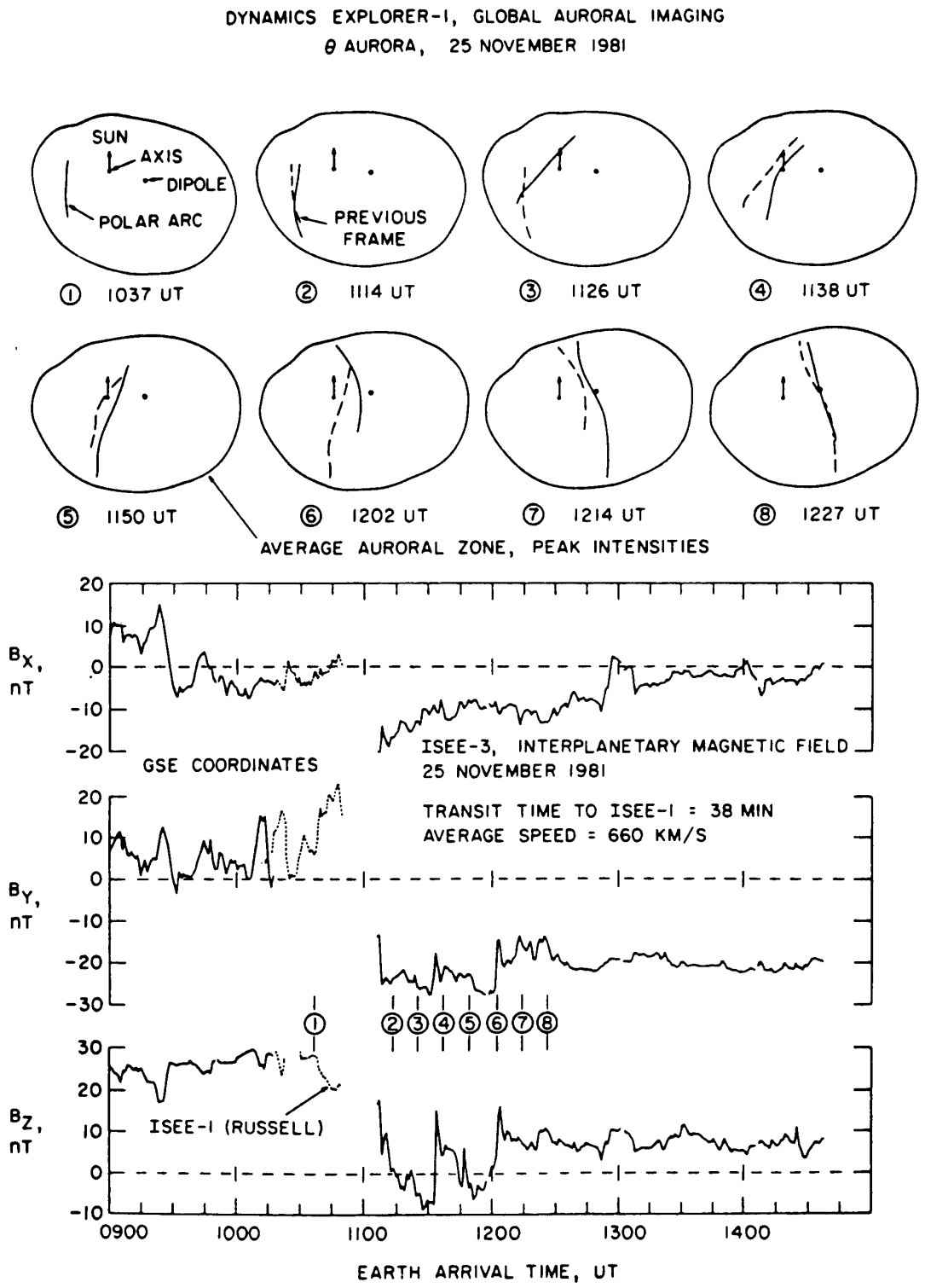

Fig. 14b. Example of the 'polar cap arc' by Dynamics Explorer and the simultaneous IMF observation (FRANK et al., 1985).

situation is shown in Fig. 15, which illustrates schematically auroral conditions during the maximum epoch of a substorm. Figure 16 shows two photographs of the afternoon-evening half of the auroral oval over the Antarctic region; one can see that day-

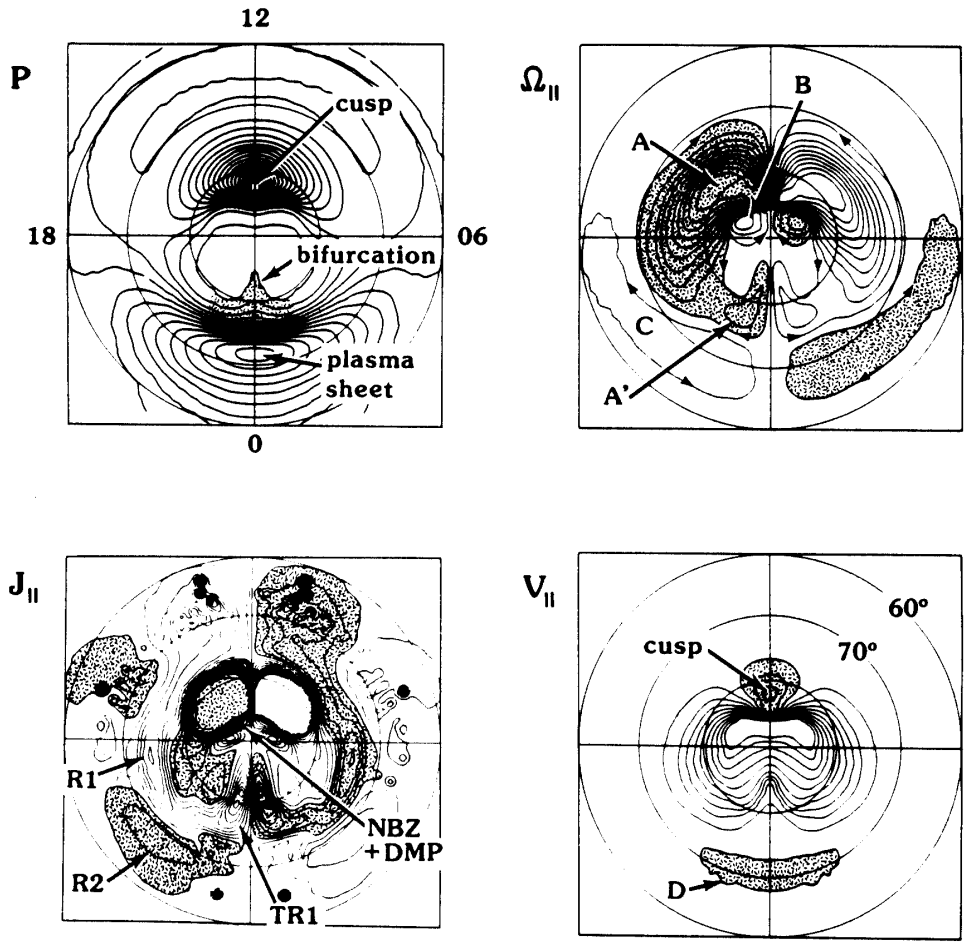

Fig. 14c. Projections of the plasma pressure, p, field aligned vorticity, $\Omega_{\parallel}$, field aligned current, $J_{\parallel}$, and field aligned velocity, $V_{\parallel}$ along magnetic field lines to the northern hemisphere of the Earth for a northward IMF of $B_z = 5$ nT. The quantities $\Omega_{\parallel}$, $J_{\parallel}$, and $V_{\parallel}$ are parallel to the magnetic field in the shaded regions and antiparallel in the open regions. The plasma sheet projection extends into the northern lobe in the region around midnight. The region 1 (R1), tail lobe region 1 (TR1), northern B_z (NBZ) and dayside magnetopause (DMP) field aligned currents are seen on the $J_{\parallel}$ plot.

side arcs are not connected to nightside arcs. AKASOFU and KAN (1980) noted that during quiet periods (IMF $B_z > 0$) the dayside arc system remains often fairly bright even if the night arc system fades (becoming below the DMSP imager threshold). It may be of interest to examine whether or not the region occupied by the dayside arc system during such a situation ($B_z > 0$) coincides sometimes with the crescent shape region for the IMF $B_x > 0$ (see Fig. 6b).

5.5. *Effects of the northward turning of the IMF B_z and substorms*

One of the most prominant features of auroral substorms is the poleward expansion of active auroras in the midnight sector. On the other hand, the northward turning of the IMF B_z component will reduce the area of the open field line region. Therefore, as the IMF B_z component is turning northward, there will be a poleward motion of auroras. In the next section, we shall see that the electron precipitation region expands also poleward as the IMF B_z component becomes positive. Therefore,

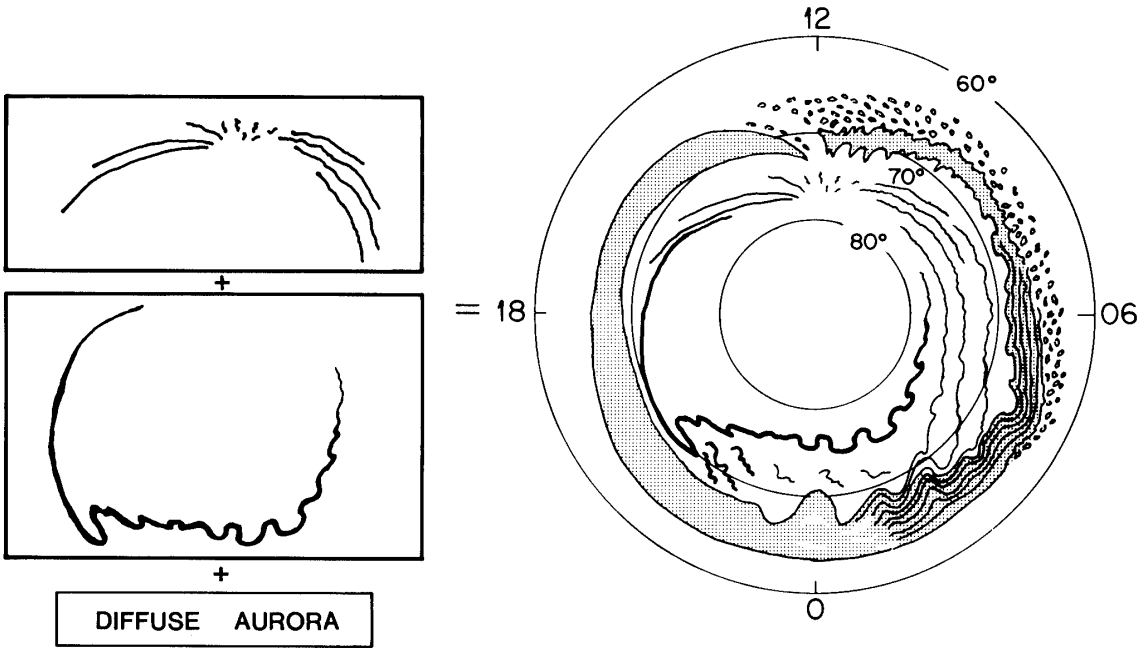

Fig. 15. Schematic illustration of the distribution of the aurora, indicating that the oval consists of the dayside and nightside arc systems (AKASOFU, 1976).

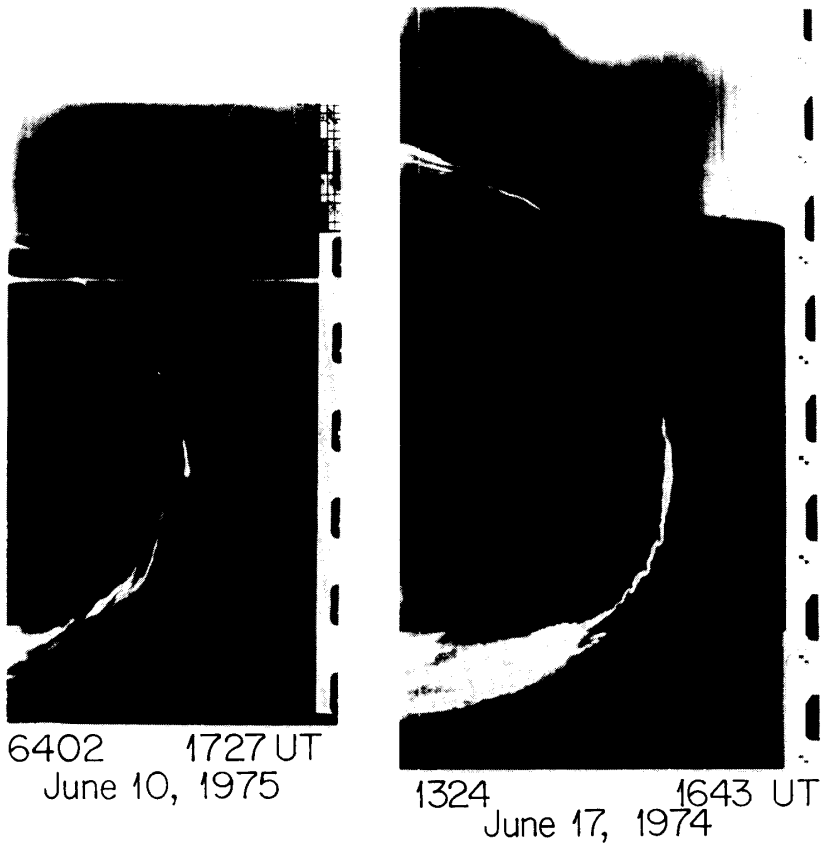

Fig. 16. DMSP images of the afternoon-evening half of the auroral oval, indicating that the dayside and nightside arcs are not connected.

the poleward motion of the auroral arcs associated with the IMF B_z northward turning may resemble sometimes the poleward expansion of auroral arcs during the expansive phase of auroral substorms. In some cases, the northward turning may indeed trigger a substorm. In this regard, it is interesting to note that ROSTOKER (1983) examined the triggering of the expansive phase of substorms by the northward turning of the IMF, although such substorms do not occur very frequently.

6. Auroral Electron Precipitation

Most auroral electron detectors in the suitable energy range can detect electron fluxes well below the level they can produce luminosity observed by auroral imaging devices. Thus, a study of changes of the electron precipitation pattern caused by the IMF has some advantage compared with a study of changes of auroral distribution. Therefore, we examine changes of the distribution of precipitating electrons, for $B_z \gtrless 0$ and $B_y \gtrless 0$.

As a polar orbiting satellite traverses across the polar region along a dawn-dusk orbit, it crosses the auroral oval twice, once in the evening sector and the other in the morning sector. For example, as the satellite advances into higher latitudes from the dusk side, it will see the so-called 'hard precipitation region' and then the 'soft precipitation region' at a little higher latitude. Then, after crossing the highest latitude region, the satellite crosses first the 'soft precipitation region' and then 'hard precipitation region' in the lower latitude side. For the IMF $B_z \sim 0$, both precipitation regions are located approximately where the oval is located, namely between $\sim 65°$ and $\sim 75°$. However, as the magnitude of the $B_z > 0$ component increases for several hours, there occurs a spectacular change. Figure 17 is such an example (MAKITA and MENG, 1984). The soft precipitation region expands poleward and tends to fill almost completely the area bounded by the pre-existing soft precipitation region (MENG, 1981b; MAKITA and MENG, 1984; HARDY, 1984). In the lower part of Fig. 17, both precipitation zones are marked along the satellite orbit. In this particular example, one can see that the soft precipitation region is present everywhere, except for a small area above invariant latitute $\sim 85°$. In Fig. 6a, we found that such a situation could occur for $B_x > 0$ and $B_z > 0$. On the other hand, as soon as the IMF B_z component becomes negative, the width of the soft precipitation region becomes drastically reduced. The corresponding changes of the hard precipitation (for the corresponding IMF changes, see Fig. 19) region is relatively very small. Figure 18 shows an example of this change. One can see that the poleward boundary of the soft precipitation region shifted from 83.6° to 80.8° in the morning sector, while it shifted from 80.3° to 71° in the evening sector.

On the basis of DMSP particle and image data and the simultaneous all-sky photographs from the South Pole station, MAKITA *et al.* (1983) demonstrated that the soft precipitation region produces a faint glow. Thus, the soft precipitation produces luminosity which is too faint to be registered by the DMSP image (particularly with snow-covered background), but can be recorded by a high sensitivity all-sky camera. A network of ground-based photometers (preferably all-sky photometers; see Section 9) will have no difficulty in studying this phenomenon.

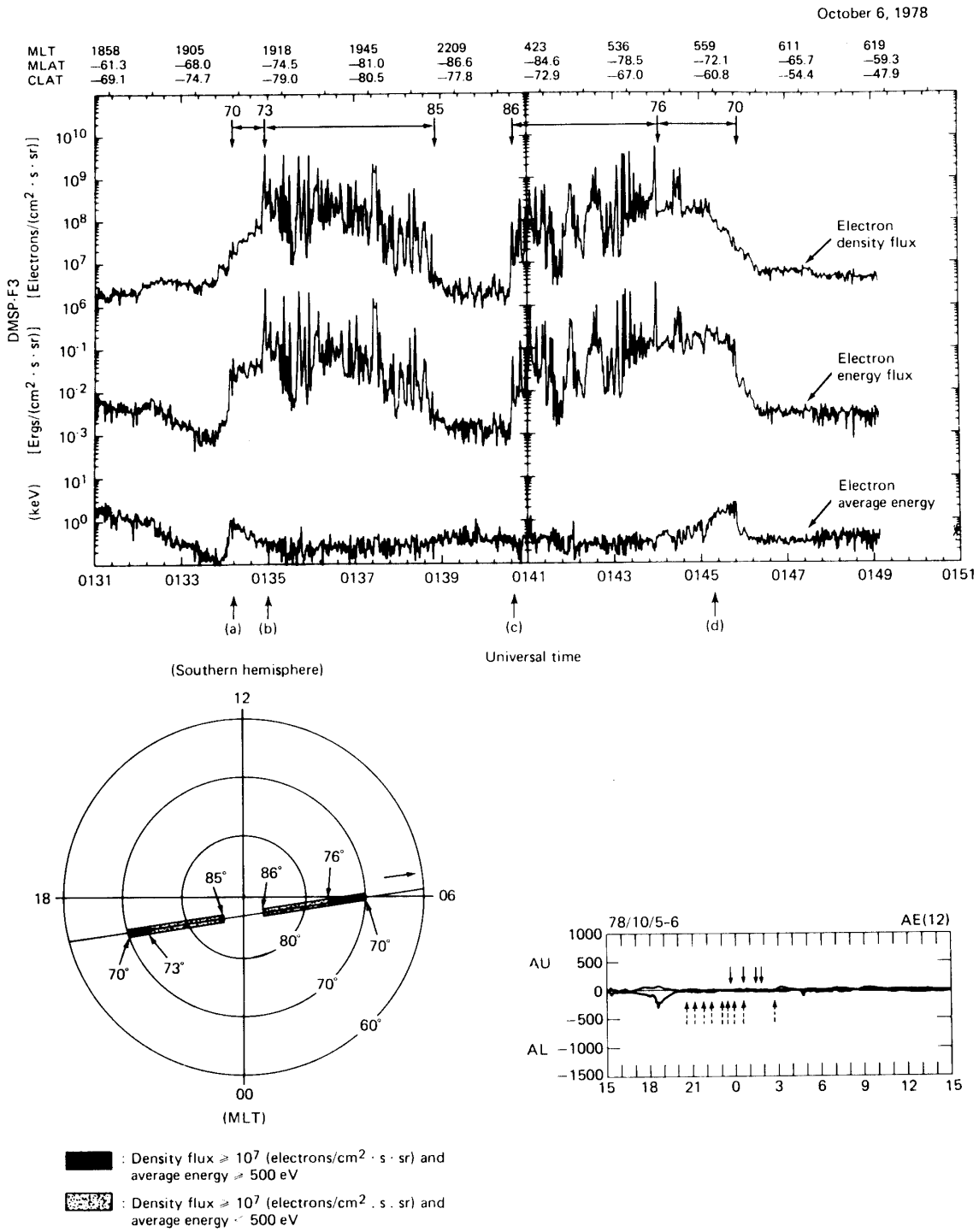

Fig. 17. Dawn-dusk profile of the electron density flux, energy flux and average energy during a very quiet period. The satellite (DMSP) orbit and the AU/AL index are also shown (MENG, 1981b).

Thus, as a first approximation, the soft precipitation region grows and decays as the IMF B_z component turns northward and southward. This must be a manifestation of a very major structural change in the magnetosphere. It has long been known that the thickness of the plasma sheet tends to be large during quiet periods, so that the

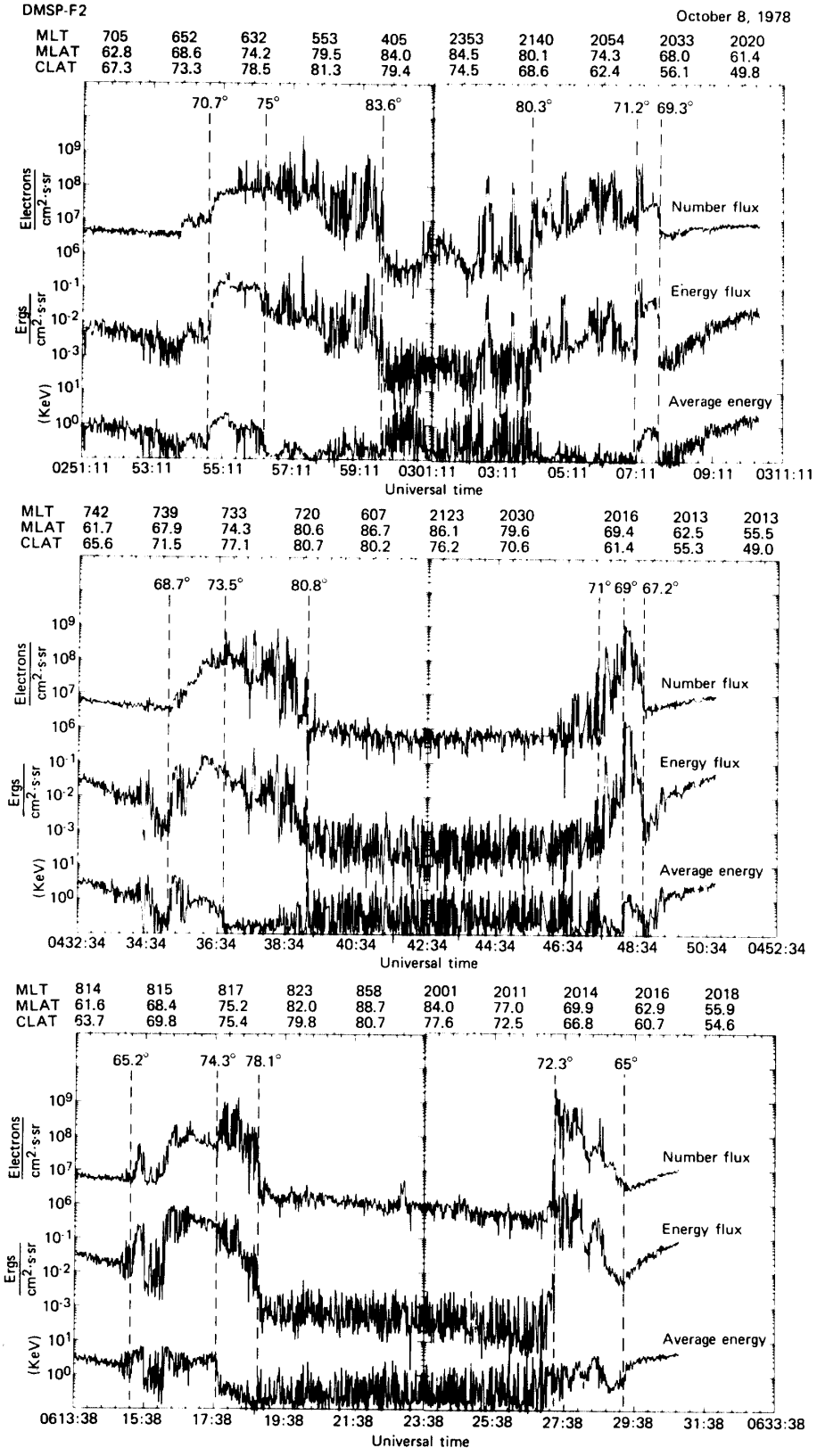

Fig. 18. Three successive profiles of the electron precipitation characteristics (for the format see the caption for Fig. 17) (MAKITA et al., 1985).

changes of the soft precipitation region must indeed be a manifestation of these plasma sheet variations (MENG, 1981a). However, two important questions arise in this connection: From where do these plasma particles come and where do they go when the IMF B_z component turns southward? This question will be discussed after we learn how the amount of the open flux varies during substorms.

MAKITA *et al.* (1985) examined also overall changes of the precipitation regions for a number of substorms. Figure 19 shows changes of the distribution of the precipitation regions during a substorm which was associated with a southward turning of the IMF vector, resulting in an increase of the dynamo power ε. One can see that as the IMF B_z component turned southward at the libration point ($\sim 250 R_E$ upstream of the solar wind), the distance between the poleward boundaries of the dawn and dusk soft precipitation regions began to expand equatorward about one hour later, namely when the IMF B_z 'signal' arrived at the magnetosphere. An important point to make here is that the expansion had begun well before the *AE* index began to in-

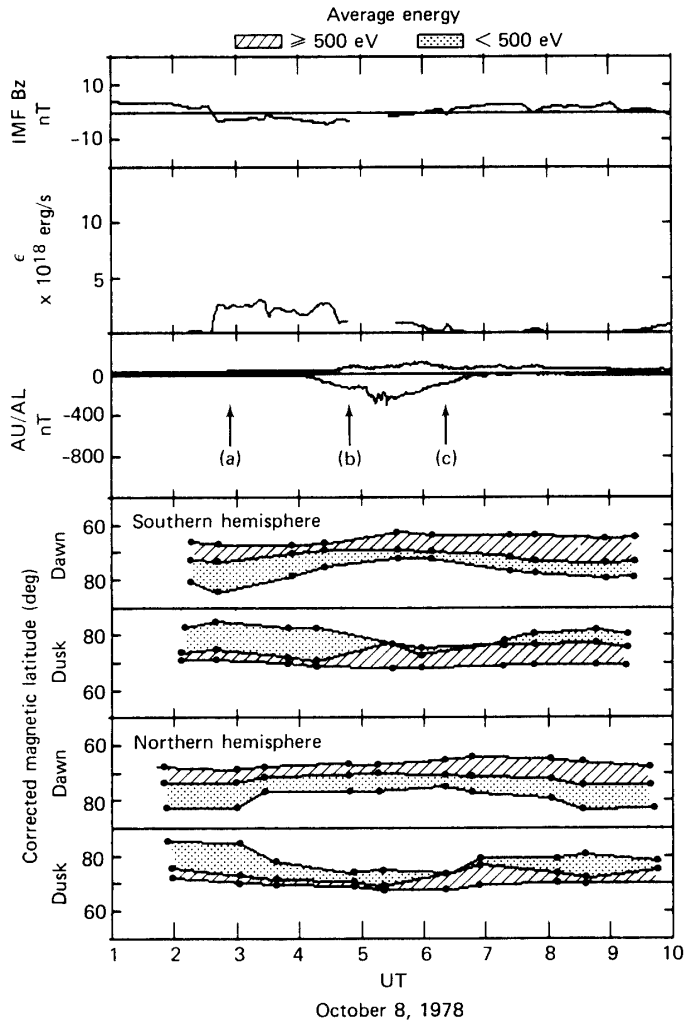

Fig. 19. Changes of the dawn-dusk precipitation profiles in both hemispheres during the early half of October 8, 1978; the soft zone and hard zones are distinguished. The corresponding IMF B_z component, the dynamo power ε and the AU/AL index are shown (MAKITA et al., 1985).

crease and that the expansion reached the maximum at about the time when the *AE* index reached the maximum value. MAKITA *et al.* (1985) showed that similar changes occur along the noon-midnight meridian as well; see also CRAVEN and FRANK (1985).

Assuming that the dawn-dusk dimension of the region of precipitation absence gives a reasonable measure of the 'diameter' of the open field line region, one can infer that the amount of the open magnetic flux increases and decreases in harmony with the *AE* index. That is to say, the amount of the open magnetic flux is not reduced to a minimum value at the peak of a substorm.

This observation has a far reaching consequence in understanding magnetospheric substorms. It has long been thought that magnetospheric substorms are caused by explosive magnetic reconnection, converting suddenly magnetic energy (stored in the magnetotail prior to substorm onset) into substorm energy. If this would indeed be the case, we would expect a large reduction of the open flux during the expansive phase of substorms storms and thus of the 'diameter' of the open field region. Therefore, for this reason, it is likely that the magnetospheric substorm is not caused entirely by explosive magnetic reconnection, but by a directly driven and other processes externally by the solar wind. In fact, the *AE* index is known to be correlated well with the IMF B_z component (or VB_z, V^2B_z, ε etc, where V denotes the solar wind speed and ε denotes the solar-wind magnetosphere dynamo power determined by PERREAULT and AKASOFU (1978)), indicating that the *AE* index (a substorm parameter) is well controlled *externally* by the solar wind as a first approximation, not internally by some unknown magnetospheric processes.

Now, as we have seen, the amount of the open flux increases during substorms. Since we know that the 'diameter' of the magnetotail is determined by the ram pressure of the solar wind, the increased open flux must be accommodated in the same cross section of the magnetotail (unless the ram pressure happens to change at the southward turning of the IMF). It is not difficult to infer that the increased open flux will squeeze out the plasma in the plasma sheet, explaining most naturally the thinning of the plasma sheet during substorms; it is known that the thinning is not compression. Indeed, HONES *et al.* (1972) demonstrated that the protons in the plasma sheet appear in the magnetosheath during substorms. It is expected that the opposite process will take place when the open flux is reduced as the IMF B_z component turns northward. In fact, the plasma sheet is known to expand during the 'recovery phase' of substorms, implying that the IMF B_z component turns northward.

7. Convection

7.1. *IMF $B_z>0$ effects*

It has been well established that there is a large-scale convection in the magnetosphere (AXFORD and HINES, 1961). In the ionospheric level, the convective flow pattern consists of two vortices, one located in the evening sector and the other in the morning sector. The potential drop across the open field line is responsible for driving the convection. The total (dawn-dusk) potential drop Φ_{pc} is a function of ε or more likely of $\sqrt{\varepsilon}$ (REIFF *et al.*, 1981; see also DOYLE and BURKE, 1983); see Fig. 20. In each vortex, there is a line across which the flow direction changes, from the anti-

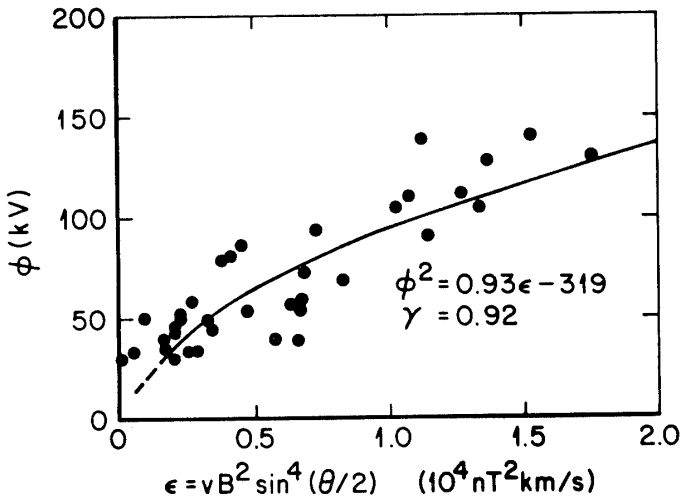

Fig. 20. Relationship between the dawn-dusk potential drop Φ_{pc} and the solar wind-magnetospheric dynamo power ε (REIFF et al., 1981).

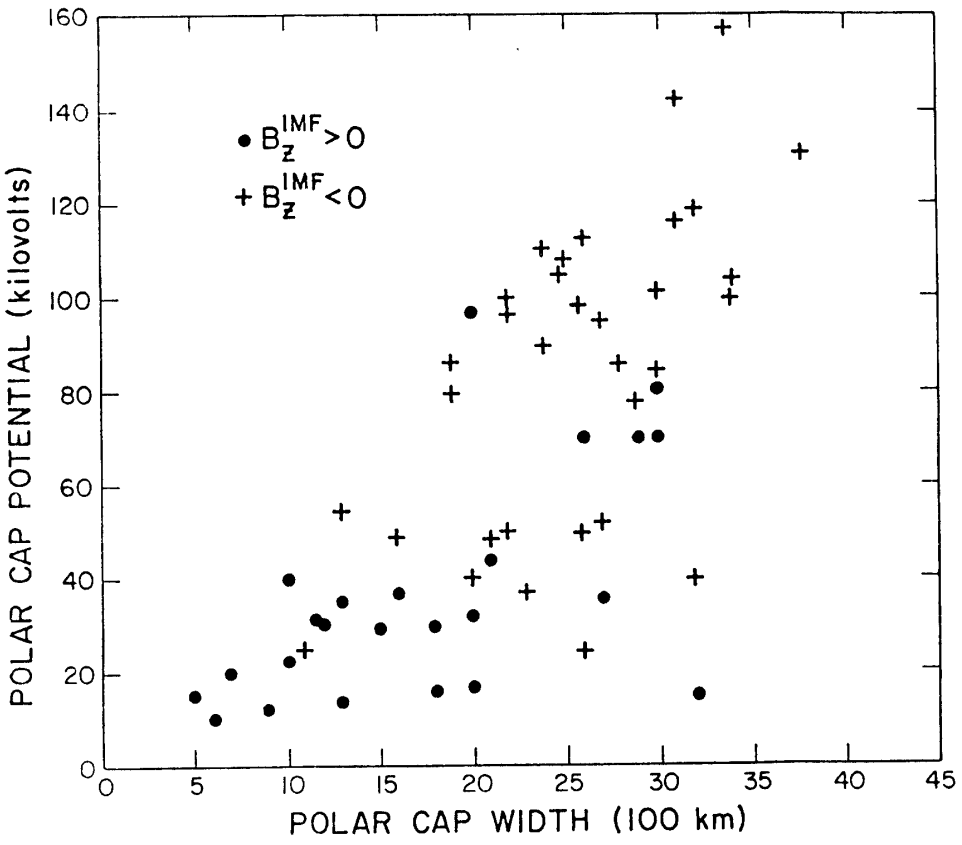

Fig. 21. Relationship between the dawn-dusk potential drop and the distance between the dawn-dusk reversal line (WYGANT et al., 1983).

sunward flow in the higher latitude side to the sunward flow in the lower latitude side. This line is often referred to as the 'convection reversal line'. The distance between the dawn and dusk reversal lines is related to the dawn-dusk potential drop (WYGANT *et al.*, 1983); see Fig. 21. That is to say, when the total potential drop is large, the

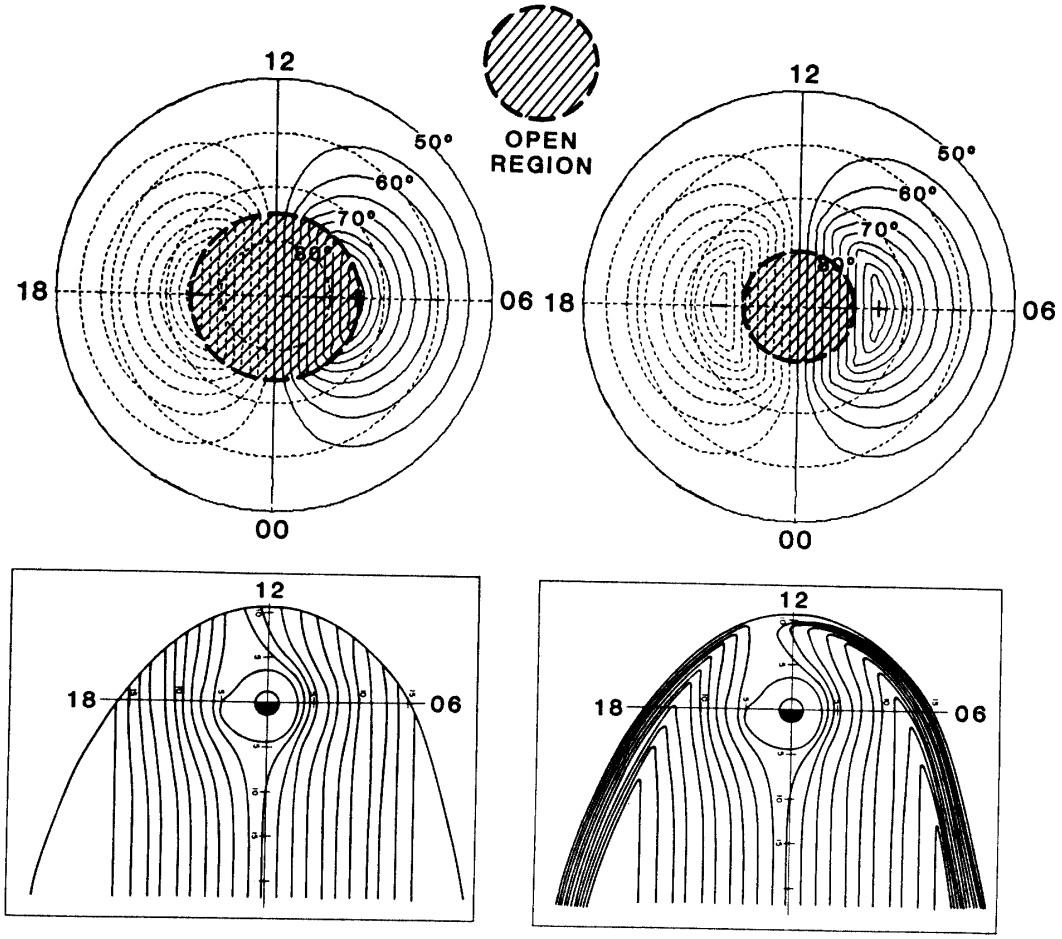

Fig. 22. Two possible relationships between the open field line region and the convection pattern in the polar region. The corresponding convection patterns in the equatorial plane MOZER, *1984) are also shown.*

open flux will also be large.

There is at least one crucial unsolved problem in this general pattern. The question is where the twin vortex is located with respect to the open field line region (*cf.* MOZER, 1984). Two possibilities are schematically illustrated in Fig. 22. It has been a long held view by a number of workers that the 'convection reversal line' should be co-located with the boundary of the open field lines region. If this would indeed be the case, the 'convection reversal line' should coincide with the poleward boundary of the auroral oval. However, there have already been some observations that the 'convection reversal line' is embedded within the electron precipitation region, indicating that the two boundaries do not coincide (HEELIS *et al.*, 1980). If this is indeed the case, the 'convection reversal line' may not necessarily delineate the boundary of the open field line region. Therefore, until this uncertainty can be clarified, one must be cautious in identifying the 'convection reversal line' and the precipitation boundary as the boundary of the open field line region.

From Fig. 22, one can see that this problem is also related to the convection flow pattern in the equatorial plane. If the two boundaries would coincide, the sunward convection flow lines should reach the magnetopause directly. However, if the two

boundaries would not coincide, the sunward convection flow from the nightside should reverse the direction near the boundary, suggesting the presence of a layer near the magnetopause, in which the flow is directed anti-sunward. It remains to be seen whether or not the boundary layer coincides with such a layer. There have been some suggestions that the convection is driven by a viscous-like process (AXFORD and HINES, 1961; REIFF, 1984), even if the magnetosphere is practically closed (namely when the IMF B_z is positive and large).

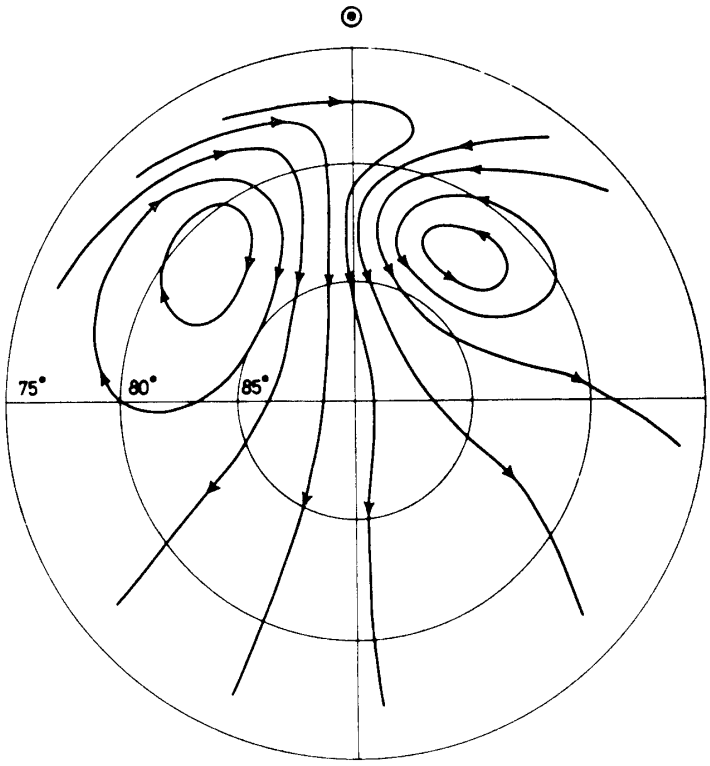

Fig. 23. Convection pattern in the polar region for the IMF $B_z>0$ (MEAZAWA, 1976).

It appears that the convection pattern becomes decidedly more complex when the IMF B_z component turns northward. The resulting changes of the convection pattern may not be a simple contraction and a weakening of the flow pattern for the IMF $B_z<0$. MAEZAWA (1976) was the first to recognize that the convection direction is reversed in the highest latitude region during quiet periods. His results are reproduced as Fig. 23. HORWITZ and AKASOFU (1979) suggested that there may be four vortices, instead of two, appearing in such a situation. BURKE *et al.* (1978, 1980, 1984) showed a satellite observation which is suggestive of the presence of four vortices; see Fig. 24. The uncertainty of the convection pattern is further complicated by not enabling us to determine the boundary of the open field line region. As stressed earlier, the boundary of the open field line region provides the natural coordinate system in magnetospheric physics. BURKE *et al.* (1978, 1980, 1984) found also that the four-cell pattern is clearly seen only in the sunlit polar region; the electric field in Fig. 24 was observed in the southern hemisphere in December. In the dark polar region, the electric field (along satellite orbits) is very irregular. This is a puzzling, but an in-

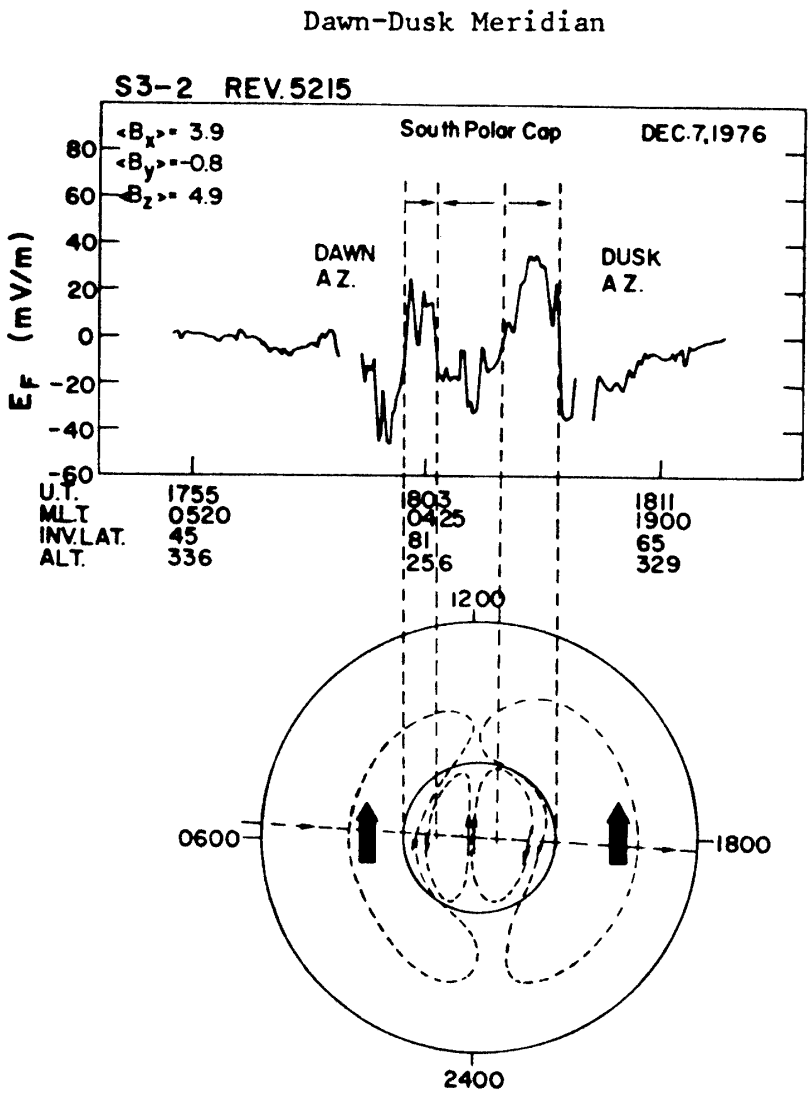

Fig. 24. Dawn-dusk electric field profile and the inferred four-cell convection pattern in the sunlit (southern) polar region (BURKE et al., 1978).

teresting problem. In Fig. 25, the convection pattern proposed by KAN and BURKE (1985) is shown. The authors have suggested that the convection (and thus the potential) pattern develop irregularities during period of the IMF $B_z>0$.

From the above discussion, one can easily see that there are still a number of fundamental issues left unsolved in a study of the convection pattern. Either or both ground-based and satellite observations are needed to elucidate the convection pattern during a prolonged period of the IMF $B_z>0$. One serious drawback of satellite observations in this regard is that the elective field (though *in situ*) is measured only along the satellite orbit, so that it is difficult to infer an instantaneous flow pattern over the entire polar region. The present ground-based measurements are limited in the 'field of view' or time or both.

7.2. *IMF B_y effects*

The dependence of the convection pattern on the IMF B_y component has been

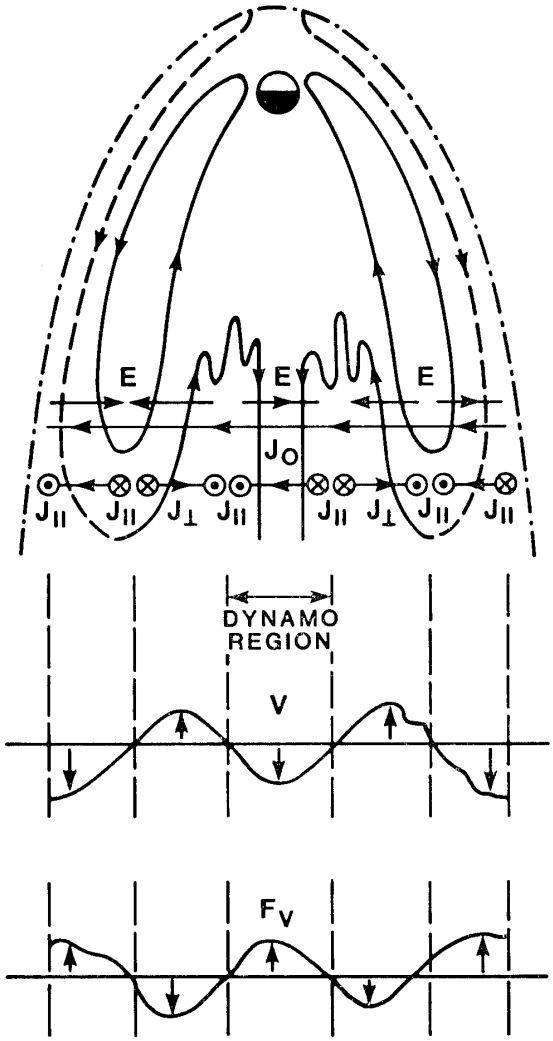

Fig. 25. Convection pattern proposed by KAN and BURKE (1985).

known for some time (HEPPNER, 1977). However, his results were based on data from a satellite which remained close to along the dawn-dusk meridian. HEELIS and HANSON (1980), WYGANT *et al.* (1983), HEELIS (1984), BURCH *et al.* (1985), and REIFF and BURCH (1985) used satellite data which have much wider spatial coverage; see also DE LA BEAUJARDIERE *et al.* (1985). In particular, WYGANT *et al.* (1983) showed that the area of the anti-sunward convection is located in the open field line region determined by the modeling in Section 3. Thus, we have a reasonably accurate knowledge on the effects of the IMF $B_y \gtrless 0$ on the convection pattern. There has also been some theoretical work on this subject (COWLEY, 1981a, b, 1982a, b).

It should be emphasized also that at the present time there is no operating method which monitors continuously the convection flow since incoherent scatter radars have only intermittently been operated. It will be a great contribution to magnetospheric physics if the convection can be monitored in the Antarctic region *on a continuous basis.* In this connection, it is worthwhile to examine the possibility of operating the classical radio 'drift' method for this purpose with one central transmitter and

several receiving stations. In the highest latitude region, this method would not suffer from heavy absorption which is a great drawback in the auroral zone. This method will also be much less expensive than an incoherent scatter radar observation.

8. Ionospheric Currents and Field-Aligned Currents

8.1. Ionospheric currents

Ionospheric currents are closely related to the magnetospheric convection, but it is worthwhile to examine the current patterns somewhat independently from the convection pattern. This is partly because ground-based magnetometers and advanced computer algorithms have recently become a powerful tool in obtaining the distribution of electric currents over the entire polar region (MISHIN *et al.*, 1980; KAMIDE *et al.*, 1981; AHN *et al.*, 1984). It has long been known that there appear two concentrated ionospheric currents: the westward electrojet in the morning sector and the eastward electrojet in the evening sector. The current distribution is relatively simple during substorms. However, our knowledge of the current distribution during prolonged periods of the IMF $B_z>0$ is very poor at the present time. It may well be that a significant part of the current system during such a period is confined to the sunlit part of the cusp region.

It has been suggested by a number of workers that a twin vortex current (or the so-called 'DP-2' current system) forms in the highest latitude region during quiet periods and prior to the onset of the expansive phase of substorms and that the two electrojet current system (or the so-called 'DP-1' current system) grows as the expansive phase develops (NISHIDA, 1978; TROSHICHEV, 1982; NISHIDA and KAMIDE, 1983). However, such results were based on a study of the distribution of the *equivalent* current vectors at a rather limited number of stations. AHN *et al.* (1984) examined the growth and decay of the *true* ionospheric currents (rather than the equivalent currents) on the basis of magnetic records from 71 stations and found that the two-electrojet system constitutes the basic current distribution pattern even during a very early epoch of substorms. In fact, there is no indication that the suggested twin vortex current is the main feature. For example, in Fig. 26, the presence of the westward and eastward electrojet at 1040 UT on March 17, 1978 is evident, while the *AE* index at that time (though not shown here) showed no indication of substorm activity. Therefore, although the twin vortex current (the Hall current) may be expected from the twin vortex convection pattern, a poor conductivity in the highest latitude region, together with the presence of the Pedersen current, alters considerably the actual current distribution, so that the twin vortex current pattern is masked by the electrojet system even during the earliest epoch of substorms. In fact, AHN *et al.* (1984) showed that the two electrojets are present even before the *AE* index begins to show the sign of a substorm. This implies also that the *AE* index fails to monitor an early phase of substorms, because the magnetic observations contributing to the *AE* index are located well equatorward of the area where the initial activity begins.

It is thus of interest to examine magnetic variations at stations above $\sim 80°$ in latitude during fairly quiet periods. For this purpose, we have chosen Thule (86.1°), Resolute (83.2°) Mould Bay (79.6°) and Godhaven (79.4°) and superposed the total

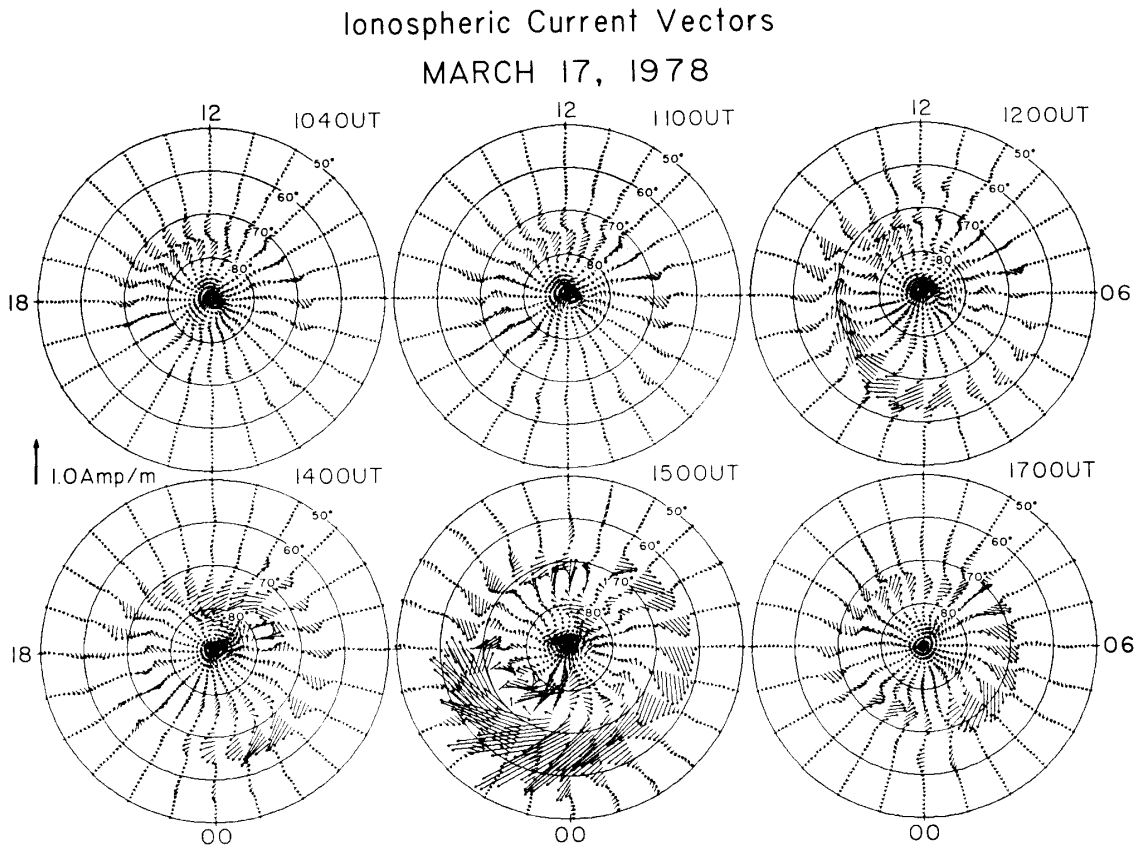

Fig. 26. Growth and decay of ionospheric currents during a substorm on March 17, 1978 (AHN et al., 1984).

horizontal component variations $B_T=(\sqrt{B_x^2+B_y^2})$ traces by selecting several quiet days (Figs. 27a and 27b). We plot also the *AE* index and the simultaneous solar wind-magnetosphere dynamo power ε in the middle and lower parts, respectively. It can be seen that the total horizontal variations B_T can respond well to ε variations of less than 10^{17} erg/s and less, while the *AE* index responds to ε values $\sim 6\times 10^{17}$–1×10^{18} erg/s and above. In fact, KOKUBUN (1971) showed earlier that the time lag between the IMF B_z and the *PC* index is significantly shorter than that between the IMF B_z and the *AE* index. Note also that another reason for B_T to be able to monitor small ε changes is that the noise level is rather low ($\sim$20 nT in the highest latitude regions), while the *AE* index (in the auroral zone) has the "noise level" of the order of 100 nT; here, by the "noise level", we mean residual incertainty of the subtraction of the daily variations.

It may be recalled that we examined earlier the relationship between the diameter of the open field line region (determined by the auroral electron precipitation) and the *AE* index, as well as with ε and the IMF B_z. There is little doubt that all these results, together with the *PC* index study, can be interpreted that the IMF B_z southward turning (or an increase of ε above 6×10^{17} erg/s) causes an expansion of the open field line region from a very high latitude ($\geqq 80°$) to lower latitudes. The aurora will brighten and the two-electrojet system will also be intensified. However, such early effects cannot be monitored well at the standard auroral zone stations, including the

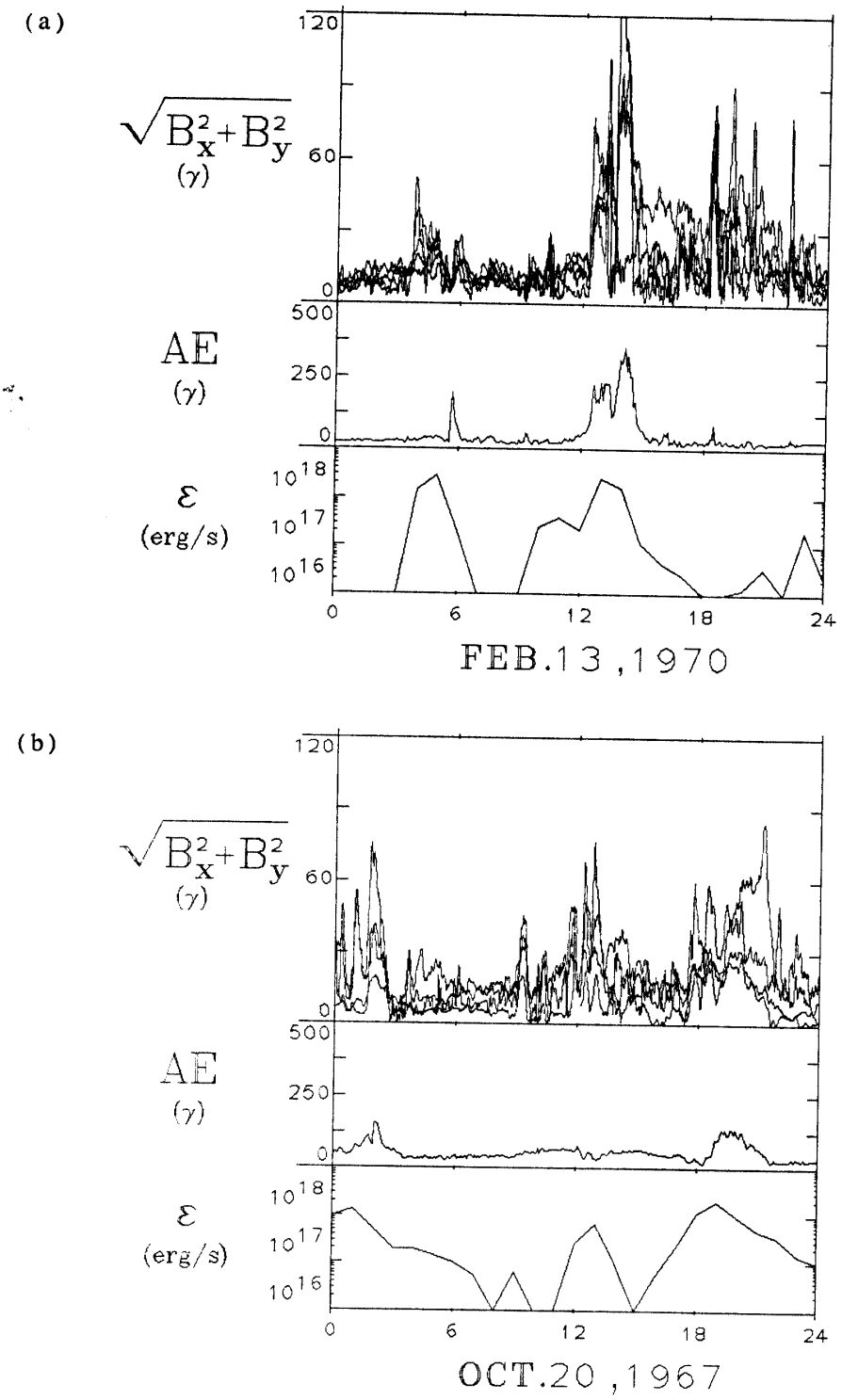

Figs. 27a and 27b. Superposed total horizontal magnetic variations at four high latitude stations, the AE index and solar wind-magnetosphere dynamo power on February 13, 1970 (a) and October 20, 1967 (b).

AE index stations.

In this regard, one may recall that a significant delay (30–45 min) of the onset of substorms after the southward turning of the IMF B_z has been considered as a crucial

fact that energy for a magnetospheric substorm is being stored for a sudden release. However, it is most likely that such a conclusion is based on unawareness of the immediate responses of the magnetosphere, which take place in the highest latitude region as we discussed in the above. Furthermore, the auroral brightening and the development of the electrojet implies a significant dissipation of the power (ε) generated by the solar wind-magnetosphere dynamo even during this period. Therefore, the 'delay period' is neither the intrinsic delay period, nor a simple energy storing period. An important point to make here is that such highest latitude observations are crucial in identifying the basic processes associated with the interaction between the solar wind and the magnetosphere. A close network of highest latitude observatories in the Antarctic region will be able to contribute significantly in clarifying a number of fundamental issues in magnetospheric physics.

The IMF B_y dependence on the daily magnetic variations and the ionospheric currents pattern has extensively been discussed in the past (SVALGAARD, 1973; ROSTOKER, 1980). In general, in the northern hemisphere, there is a tendency for the east-west directed current to be enhanced in the morning sector for the IMF $B_y>0$ and in the evening sector for the IMF $B_y<0$. There is little doubt that these tendencies are closely related to changes of the convection pattern. However, the ionospheric current depends not only on the potential (electric field) distribution, but also on the conductivity which depends, in turn, on the flux of precipitation electron flux.

8.2. Field-aligned currents

It is well established that the field-aligned current system consists of Region 1 and 2 currents (IIJIMA and POTEMRA, 1976, 1978). A part of the field-aligned currents is fed from the magnetosphere, generating ionospheric currents. Another part of the field-aligned currents may be generated in the ionosphere and leaks out into the magnetosphere. The distribution obtained by IIJIMA and POTEMRA (1976), represents a weak to moderate substorm condition, namely for a period of a weak negative IMF B_z component. It is perhaps difficult to determine the dependence of the distribution of the field-aligned currents on the IMF B_y component; like the other polar upper atmospheric phenomena, such effects are likely to be masked by effects of the IMF B_z component.

It is only recently that the distribution of the field-aligned currents during prolonged periods of the IMF B_z component has been examined extensively. IIJIMA *et al.* (1984), POTEMRA *et al.* (1984), ZANETTI *et al.* (1984), and ARAKI *et al.* (1984) showed that there appears a field-aligned current system in the sunlit side of the region bounded by Region 1 and 2 currents. It appears to be significantly different from the Region 1/2 system and in fact becomes more intense as the IMF $B_z>0$ component becomes large. Figure 28 shows that there occurs an upward field-aligned current in the forenoon sector and a downward field-aligned current in the afternoon sector; they are an additional feature to the Region 1/2 current system. From the simultaneous electric field observation, these authors suggest the convection patterns under a variety of IMF conditions (Fig. 29).

It is one of the most challenging theoretical tasks to put together quantitatively and self-consistently the convection pattern, ionospheric currents and the field-aligned

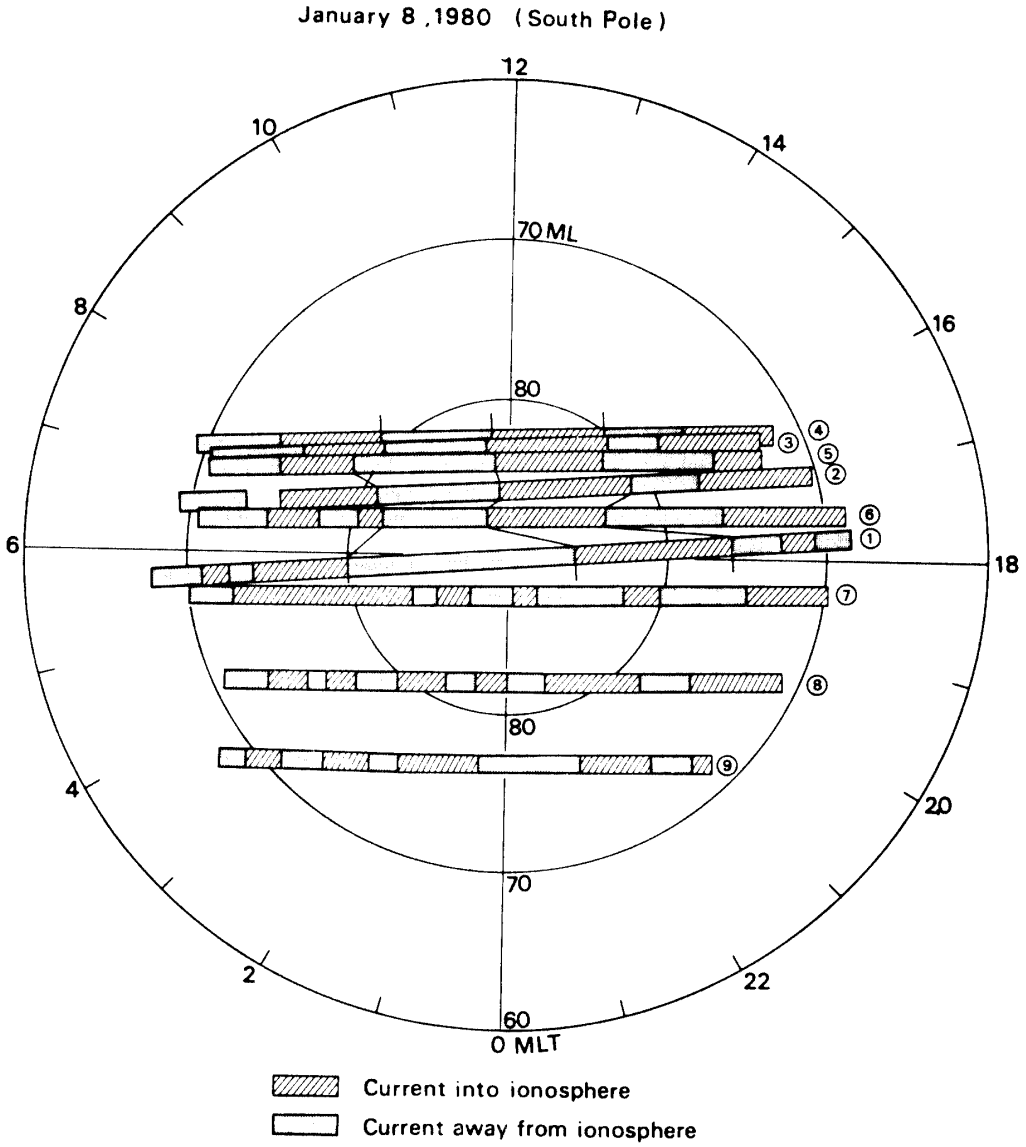

Fig. 28. Distribution of field-aligned currents during a period of the IMF $B_z > 0$ (IIJIMA et al., 1984).

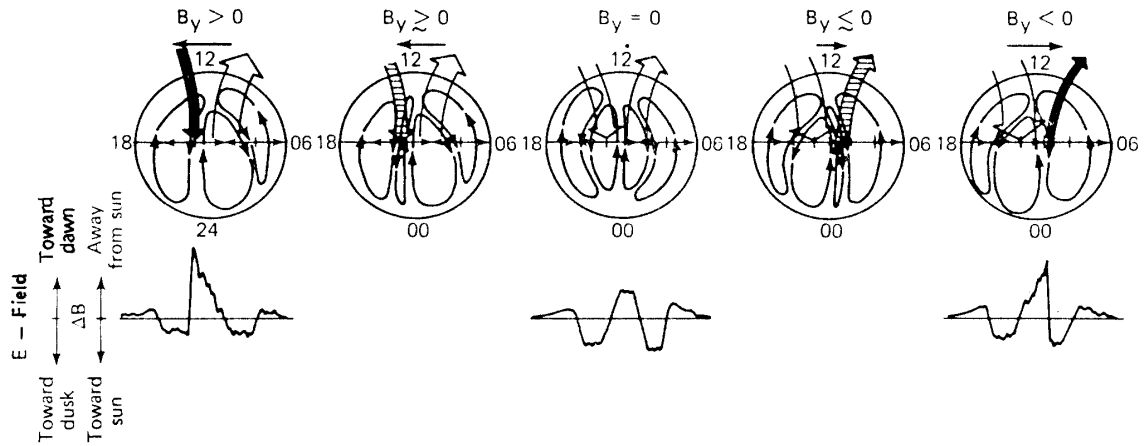

Fig. 29. Schematic illustration of the relationship between the IMF B_y component and the field-aligned current-convection; the corresponding electric field profiles along a dawn-dusk orbit are also shown (POTEMRA et al., 1984).

currents for the IMF $B_y>0$ and $B_y<0$ under the condition of the IMF $B_z>0$ (see FELDSTEIN *et al.*, 1984; OGINO *et al.*, 1984).

9. Ionosphere

All-sky imaging photometers and ionospheric soundings taken at Thule, Greenland (86°) have revealed that the winter polar cap F region is unexpectedly extremely active for both IMF $B_z<0$ and $B_z>0$ conditions. BUCHAU *et al.* (1983), WEBER *et al.* (1984), and CARLSON *et al.* (1985) showed that during quiet periods the most predominant features are sun-aligned (subvisual) F region arcs which drift from dawn to dusk or dusk to dawn at speeds 100–250 m/s. These features disappear during magnetically disturbed periods, and large patches of enhanced F region ionization drifts in the antisunward direction. Figure 30 shows schematically some of the subvisual structures.

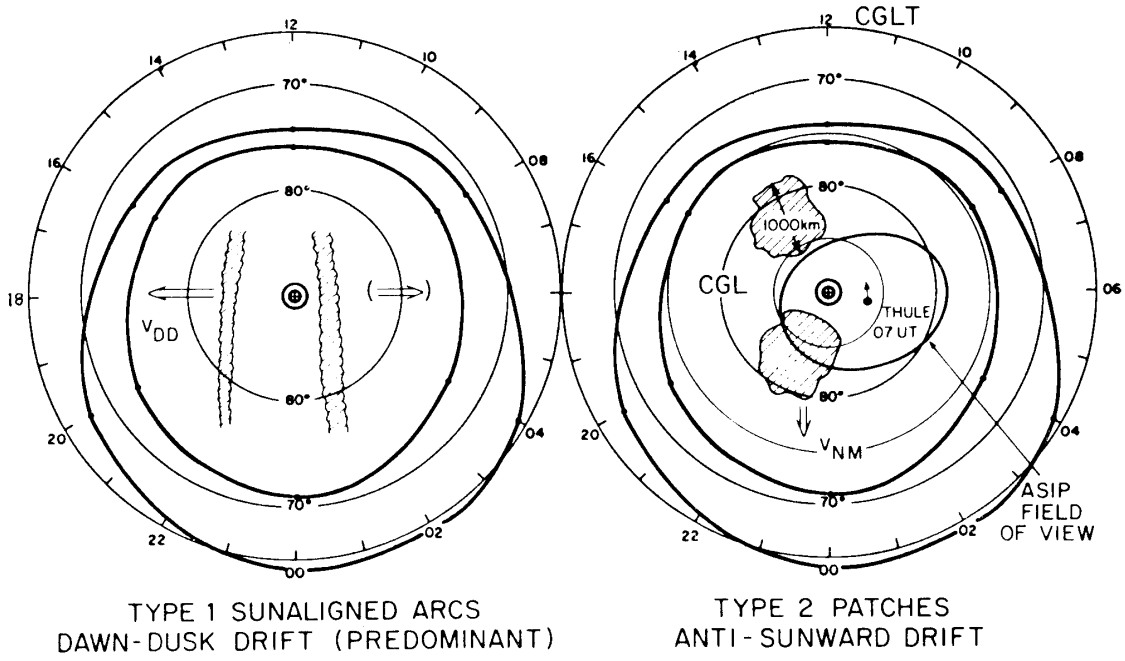

Fig. 30. Schematic illustration of the subvisual structures for different IMF conditions (BUCHAU et al., 1983).

It appears quiet certain that the plasma in the F region of the ionosphere drifts in the anti-solar direction across the highest latitude region of the earth from the dayside. This implies that a significant part of the F region ionization in the dark polar region is supplied from the dayside ionosphere by the $\boldsymbol{E}\times\boldsymbol{B}$ drift motion. Figure 31 shows an example of simulation results which demonstrate such an effect (B. WATKINS, private communication, 1984). Since the production of the ionization along the auroral oval is not included, one can see very clearly how significantly electrons in the dayside are transported into the highest latitude region.

BUCHAU *et al.* (1983) brought the most suitable set of instruments in exploring the ionosphere in the highest latitude region which has also been long ignored. There

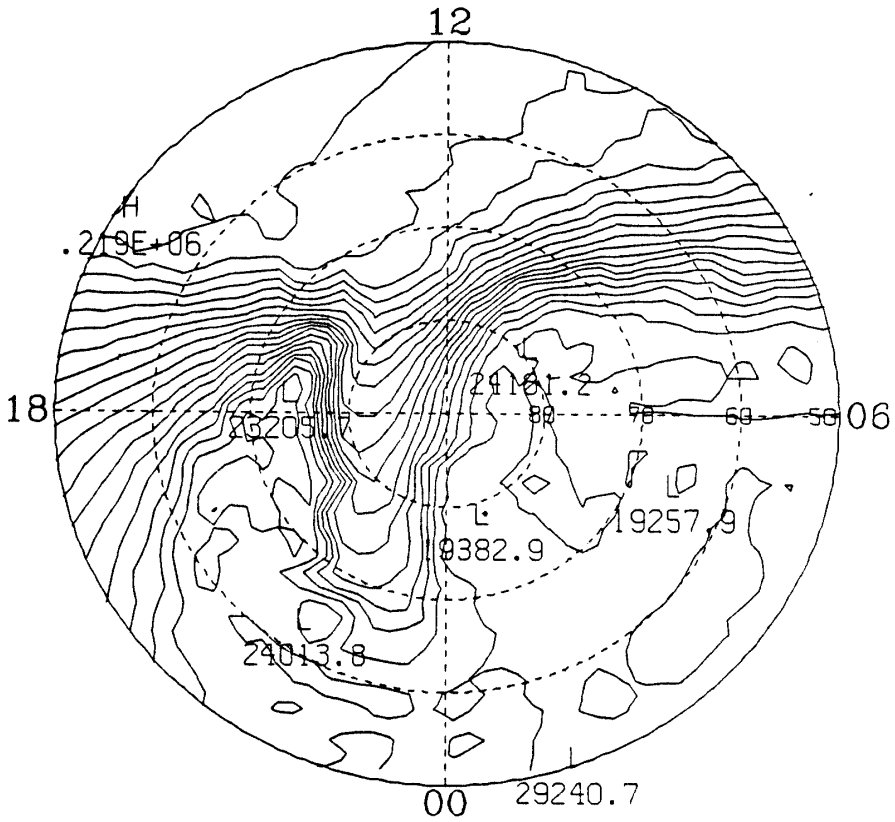

Fig. 31. Simulation of the effects of the $E \times B$ drift of the dayside ionization on the distribution of the F region in the highest latitude region of the earth (B. WATKINS, private communication, 1984).

is little doubt that the polar cap ionosphere has much to be explored further. It should be added that the ionosphere in the highest latitude region has been theoretically studied by SCHUNK and SOJKA (1982) and SOJKA and SCHUNK (1983, 1984). These authors predicted the so-called 'hot spot' or 'spots' (where the ion temperature is elevated) and several other interesting features on the basis of their simulation study. Their theoretical results have recently been compared with Millstone Hill radar results (SOJKA *et al.*, 1983).

10. Thermosphere

The winds in the thermosphere in the highest latitude region of the earth have been studied extensively by HEPPNER and his colleagues using chemical release observations (MERIWETHER *et al.*, 1973; HEPPNER and MILLER, 1982). HEPPNER and MILLER (1982) showed that the wind vector plots in the *F* region are disorganized when presented in geographic and solar local time coordinates, but are well organized when presented in magnetic local time and invariant latitude coordinates. Thus, their study suggests the dominant role of the cross-polar cap electric field which drives the anti-sunward drift motion of the ionospheric plasma which in turn drives the neutral wind in the same direction. Their study has recently been confirmed conclusively by observations by Dynamics Explorer (KILLEEN *et al.*, 1982, 1984a, b; REES *et al.*,

1983; KILLEEN and ROBLE, 1984; ROBLE *et al.*, 1984; HAYS *et al.*, 1984; EMERY *et al.*, 1985; MCCORMAC *et al.*, 1985). Figure 32 shows an example of their results. Thus, the neutral component in the *F* region of the ionosphere is forced to drift in the anti-solar direction by the $\boldsymbol{E}\times\boldsymbol{B}$ drift motion (ROBLE *et al.*, 1982).

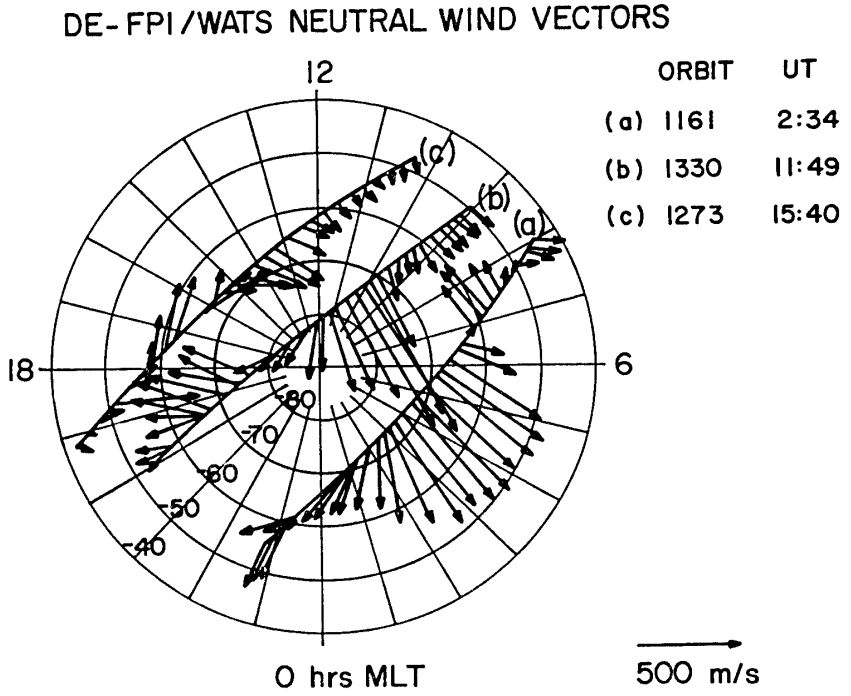

Fig. 32. Profiles of the velocity vectors of the neutral component in the F region of the ionosphere observed Dynamics Explorer (KILLEEN et al., 1982).

It remains to be seen whether or not the neutral component in the *E* region is also forced to drift by the $\boldsymbol{E}\times\boldsymbol{B}$ drift motion. Note that if the neutral component moves with the velocity $\boldsymbol{V}=\boldsymbol{E}\times\boldsymbol{B}/B^2$, the original magnetospheric electric field $\boldsymbol{E}_m$ will be cancelled by this motion in the frame of reference moving with the neutral gas, namely $\boldsymbol{E}_m+\boldsymbol{V}\times\boldsymbol{B}=0$. Therefore, even if $\boldsymbol{E}_m$ is applied to the ionosphere from the magnetosphere, there would not be ionospheric currents. Even if the neutral component moves with one half of the $\boldsymbol{E}\times\boldsymbol{B}$ drift motion, there will be a considerable reduction of the ionospheric currents. AKASOFU (1981, 1985) showed that the *AE* index tends to 'saturate' or be reduced when the dynamo power ε becomes $\sim 10^{19}$ erg/s or larger. It is of great interest to examine whether or not this tendency of the *AE* index can be explained by the forced motion of the neutral component by the $\boldsymbol{E}\times\boldsymbol{B}$ drift motion.

11. Polar Rain, Polar Wind, Hopping Motions of Heavy Ions

There are many other upper atmospheric phenomena which are characteristics of the highest latitude region of the earth. The so-called 'polar rain' is a fairly uniform precipitation of electrons of energies of ~ 20 keV in the open field line region (MENG *et al.*, 1977; GUSSENHOVEN *et al.*, 1984). These electrons are believed to be

the high energy tail portion of electrons in the solar wind (FAIRFIELD and SCUDDER, 1985). It has long been suggested that a slight polarization of the upper atmosphere arising from the ambi-polar diffusion between O^+ and electrons generates an upward flow of minor light ions H^+ and He^+ in the ionosphere. This flow is called the polar wind. Some of the ions H^+, He^+ and O^+ which are accelerated in the cusp region are ejected upward, but descend or hop in the highest latitude region (HORWITZ, 1984). These and other interesting phenomena are not described here, because ground-based observations alone would not be very useful in understanding them at the present time.

12. Conclusive Remarks

This paper is not intended to be a comprehensive review of studies of the upper atmospheric phenomena which take place in the highest latitude region of the earth, but rather be a provocative document in initiating unique and innovative observational programs in the Antarctic region; most of the earlier references not cited in this paper could be found in the cited references. Particular emphases were made in discussing those upper atmospheric phenomena which might throw some light in understanding some of the basic magnetospheric processes. It was stressed that a full understanding of the solar wind-magnetosphere interaction requires a detailed study of upper atmospheric phenomena in the highest latitude region of the earth. In the past, we have investigated mainly effects of the IMF $B_z<0$. However, much of the effects of the IMF $B_z>0$, $B_y \gtrless 0$ and $B_x \gtrless 0$ remain to be studied in the future. We have stressed in this paper that a well-organized network of conventional ground-based instruments is still a powerful tool in studying auroral phenomena which take place in the highest latitude region and can contribute considerably to a full understanding of the solar wind-magnetosphere interaction.

Acknowledgments

The author would like to thank SCAR Upper Atmospheric Group, in particular Prof. T. NAGATA and Dr. FUKUNISHI, National Institute of Polar Research and Dr. L. LANZEROTTI, Bell Laboratory, AT & T for their suggestions, discussions and encouragement during the preparation of this paper. The work reported here was supported in part by a grant from the National Science Foundation (ATM 83-12515) and by a grant from the National Aeronautics and Space Administration (NSG 7447).

References

AHN, B.-H., KAMIDE, Y. and AKASOFU, S.-I. (1984): Global ionospheric current distribution during substorms. J. Geophys. Res., **89**, 1613–1625.

AKASOFU, S.-I. (1972): Midday auroras and polar cap auroras. Geophys. Publ., **29**, 73–85.

AKASOFU, S.-I. (1976): Recent progress in studies of DMSP auroral photographs. Space Sci. Rev., **19**, 169–215.

AKASOFU, S.-I. (1981): Relationships between the AE and Dst indices during geomagnetic storms. J. Geophys. Res., **86**, 4820–4822.

AKASOFU, S.-I. (1985): A magnetospheric substorm with a nearly constant input rate for 24 hours.

Planet. Space Sci., **33**, 81–87.

AKASOFU, S.-I. and AHN, B.-H. (1980): Dependence of the amount of open magnetic flux on the direction of the interplanetary magnetic field. Planet. Space Sci., **28**, 545–547.

AKASOFU, S.-I. and COVEY, D. N. (1980): Effects of the interplanetary magnetic field on the magnetotail structure; Large-scale changes of the plasma sheet during magnetospheric substorms. Planet. Space Sci., **28**, 757–762.

AKASOFU, S.-I. and KAN, J. R. (1980): Dayside and nightside auroral arc systems. Geophys. Res. Lett., **7**, 753–756.

AKASOFU, S.-I. and ROEDERER, M. (1983): Polar cap arcs and the open regions. Planet. Space Sci., **31**, 193–196.

AKASOFU, S.-I. and ROEDERER, M. (1984): Dependence of the polar cap geometry on the IMF. Planet. Space Sci., **32**, 111–118.

AKASOFU, S.-I. and TSURUTANI, B. (1984): Unusual auroral features observed on January 10–11, 1983 and their possible relationships to the interplanetary magnetic field. Geophys. Res. Lett., **11**, 1086–1089.

AKASOFU, S.-I., COVEY, D. N. and MENG, C.-I. (1981): Dependence of the geometry of the region of open field lines on the interplanetary magnetic field. Planet. Space Sci., **29**, 803–807.

AKASOFU, S.-I., WILLIAMS, R. and ROEDERER, M. (1984): Effects of the passage of an IMF discontinuity on the polar cap geometry and the formation of a polar cap arc. Planet. Space Sci., **32**, 119–125.

ARAKI, T., KAMEI, T. and IYEMORI, T. (1984): Polar cap vertical currents associated with northward interplanetary magnetic field. Geophys. Res. Lett., **11**, 23–26.

AXFORD, W. I. and HINES, C. O. (1961): A unifying theory of high-latitude geophysical phenomena and geomagnetic storms. Can. J. Phys., **39**, 1433–1464.

BERKEY, F. T., COGGER, L. L., ISMAIL, S. and KAMIDE, Y. (1976): Evidence for a correlation between sun-aligned arcs and the interplanetary magnetic field direction. Geophys. Res. Lett., **3**, 145–147.

BUCHAU, J., REINISCH, B. W., WEBER, E. J. and MOORE, J. G. (1983): Structure and dynamics of the winter polar cap *F* region. Radio Sci., **18**, 995–1010.

BURCH, J. L., REIFF, P. H., MENIETTI, J. D., HEELIS, R. A., HANSON, W. B., SHAWHAN, S. D., SHELLEY, E. G., SUGIMA, M., WEIMER, D. R. and WINNINGHAM, J. D. (1985): IMF B_y-dependent plasma flow and Birkeland currents in the dayside magnetosphere; 1. Dynamics Explorer observations. J. Geophys. Res., **90**, 1577–1593.

BURKE, W. J., SAGALYN, R. C., SMIDDY, M., KELLEY, M. C. and LAI, S. T. (1978): Electric fields at high latitudes in the topside ionosphere near the dawn-dusk meridian. Space Res., **19**, 343–346.

BURKE, W. J., HARDY, D. A., RICH, F. J., KELLEY, M. C., SMIDDY, M., SHUMAN, B., SAGALYN, R. C., VANCOUR, R. P., WIDMAN, P. J. L. and LAI, S. T. (1980): Electrodynamic structure of the late evening sector of the auroral zone. J. Geophys. Res., **85**, 1179–1193.

BURKE, W. J., HARDY, D. A., RICH, F. J., SAGALYN, R. C., SCHUMAN, B., SMIDDY, M., VANCOUR, R., WILDMAN, P. J. L., KELLEY, M. C., DOYLE, M. A., GUSSENHOVEN, M. S. and SAFLEKOS, N. A. (1984): High latitude electrodynamics; observations from S3-2. Space Sci. Rev., **37**, 161–200.

CARLSON, H. C., WICKMAN, V. B., WEBER, E. J., BUCHAU, J., MOORE, J. G. and WHITING, W. (1985): Plasma characteristics of polar cap *F*-layer arcs. Geophys. Res. Lett. (in press).

CHIU, Y. T., CROOKER, N. U. and CORNEY, D. J. (1985): Model of oval and polar cap arc configurations. J. Geophys. Res., **90**, 5153–5157.

COWLEY, S. W. H. (1981a): Magnetospheric asymmetries associated with the *Y*-component of the IMF. Planet. Space Sci., **29**, 79–96.

COWLEY, S. W. H. (1981b): Magnetospheric and ionospheric flow and the interplanetary magnetic field. The Physical Basis of the Ionosphere in the Solar-Terrestrial System, Conf. Proc. AGARD-CP-295, Neuilly-Sur-Seine, NATO, p. 4-1.

COWLEY, S. W. H. (1982a): The causes of convection in the earth's magnetosphere: A review of

developments during the IMS. Rev. Geophys. Space Phys., **20**, 531–565.

COWLEY, S. W. H. (1982b): Interpretation of observed relations between solar wind characteristic and effects at ionospheric altitudes. (preprint)

CRAVEN, J. D. and FRANK, L. A. (1985): The temporal evolution of a small auroral substorm as viewed from high altitudes with Dynamics Explorer 1. Geophys. Res. Lett., **12**, 465–468.

DAVIS, T. N. (1962): The morphology of the auroral displays of 1957–1958; 2. Detailed analyses of Alaska data and analyses of high-latitude data. J. Geophys. Res., **67**, 75–110.

DE LA BEAUJARDIERE, O., WICKMAN, V. B., KELLEY, J. D. and KING, J. H. (1985): Effects of the interplanetary magnetic field Y component on the high-latitude nightside convection. Geophys. Res. Lett., **12**, 461–464.

DENHOLM, J. V. (1961): Some auroral observations inside the southern auroral zone. J. Geophys. Res., **66**, 2105–2111.

DOYLE, M. A. and BURKE, W. J. (1983): S3-2 measurements of the polar cap potential. J. Geophys. Res., **88**, 9125–9133.

EATHER, R. H. and AKASOFU, S.-I. (1969): Characteristics of polar cap auroras. J. Geophys. Res., **74**, 4794–4798.

EMERY, B. A., ROBLE, R. G., RIDLEY, E. C., KILLEEN, T. L., REES, M. H., WINNINGHAM, J. D., CARINGNAN, G. R., HAYS, P. B., HEELIS, R. A., HANSON, W. B., SPENCER, N. W., BRACE, L. H. and SUGUIRE, M. (1985): Thermospheric and ionospheric structure of the southern hemisphere polar cap on October 21, 1981, as determined from Dynamics Explorer 2 satellite data. J. Geophys. Res., **90**, 6553–6566.

FAIRFIELD, D. H. and SCUDDER, J. D. (1985): Polar rain; Solar coronal electrons in the earth's magnetosphere. J. Geophys. Res., **90**, 4055–4068.

FELDSTEIN, Y. I., LEVITIN, A. E., FAERMARK, D. S., AFONINA, R. G., BELOV, B. A. and GAIDUKOV, V. Y. (1984): Electric fields and potential patterns in the high-latitude ionosphere for different situations in interplanetary space. Planet. Space Sci, **32**, 907–923.

FRANK, L. A., CRAVEN, J. D., ACKERSON, K. L., CAROVILLANO, R. L. and EATHER, R. H. (1982a): Polar views of earth-global imaging with Dynamics Explorer. EOS, **63**, 386.

FRANK, L. A., CRAVEN, J. D., BURCH, J. L. and WINNINGHAM, J. D. (1982b): Polar views of the earth's aurora with Dynamics Explorer. Geophys. Res. Lett., **9**, 1001–1004.

FRANK, L. A., CRAVEN, J. D. and RAIRDEN, R. L. (1985): Images of the earth's auroral and geocorona from the Dynamics Explorer Mission. Adv. Space Res., **5**, 53–68.

GUSSENHOVEN, M. S. (1982): Extremely high latitude auroras. J. Geophys. Res., **87**, 2401–2412.

GUSSENHOVEN, M. S., HARDY, D. A., HEINEMANN, N. and BURKHARDT, R. K. (1984): Morphology of the polar rain. J. Geophys. Res., **89**, 9785–9800.

HARDY, D. A. (1984): Intense fluxes of low-energy electrons at geomagnetic latitudes above 85°. J. Geophys. Res., **89**, 3883–3892.

HARDY, D. A., BURKE, W. J. and GUSSENHOVEN, M. S. (1982): DMSP optical and electron measurements in the vicinity of polar cap arcs. J. Geophys. Res., **87**, 2413–2430.

HAYS, P. B., KILLEEN, T. L., SPENCER, N. W., WHARTON, L. E., ROBLE, R. G., EMERY, B. A., FULLER-ROWELL, T. J., REES, D., FRANK, L. A. and CRAVEN, J. D. (1984): Observations of the dynamics of the polar thermosphere. J. Geophys. Res., **89**, 5597–5612.

HEELIS, R. A. (1984): The effects of interplanetary magnetic field orientation on dayside high-latitude ionospheric convection. J. Geophys. Res., **89**, 2873–2880.

HEELIS, R. A. and HANSON, W. B. (1980): High-latitude ion convection in the nighttime F region. J. Geophys. Res., **85**, 1995–2002.

HEELIS, R. A., WINNINGHAM, J. D., HANSON, W. B. and BURCH, J. L. (1980): The relationships between high-latitude convection reversals and the energetic particle morphology observed by Atmosphere Explorer. J. Geophys. Res., **85**, 3315–3324.

HEPPNER, J. P. (1977): Empirical models of high-latitude electric fields. J. Geophys. Res., **82**, 1115–1125.

HEPPNER, J. P. and MILLER, M. L. (1982): Thermospheric winds at high latitudes from chemical release observations. J. Geophys. Res., **87**, 1633–1647.

HONES, E. W., Jr., AKASOFU, S.-I., BAME, S. J. and SINGER, S. (1972): Outflow of plasma from the magnetotail into the magnetosheath. J. Geophys. Res., **77**, 6688–6695.

HORWITZ, J. L. (1984): Features of ion trajectories in the polar magnetosphere. Geophys. Res. Lett., **11**, 1111–1114.

HORWITZ, J. L. and AKASOFU, S.-I. (1979): On the relationship of the polar cap current system to the north-south component of the interplanetary magnetic field. J. Geophys. Res., **84**, 2567–2572.

HUANG, C. Y., FRANK, L. A., CRAVEN, J. D., ELPHIC, R. C. and PARKS, G. K. (1984): High-altitude signatures of a theta aurora. EOS, **65**, 1051.

IIJIMA, T. and POTEMRA, T. A. (1976): The amplitude distribution of field-aligned currents at northern high latitudes observed by TRIAD. J. Geophys. Res., **81**, 2165–2174.

IIJIMA, T. and POTEMRA, T. A. (1978): Large-scale characteristics of field-aligned currents associated with substorms. J. Geophys. Res., **83**, 599–615.

IIJIMA, T., POTEMRA, T. A., ZANETTI, L. J. and BYTHROW, P. F. (1984): Large-scale Birkeland currents in the dayside polar region during strongly northward IMF; A new Birkeland current system. J. Geophys. Res., **89**, 7441–7452.

ISMAIL, S. and MENG, C.-I. (1982): A classification of polar cap auroral arcs. Planet. Space Sci., **30**, 319–330.

ISMAIL, S., WALLIS, D. D. and COGGER, L. L. (1977): Characteristics of polar cap sun-earth aligned arcs. J. Geophys. Res., **82**, 4741–4749.

KAMIDE, Y., RICHMOND, A. D. and MATSUSHITA, S. (1981): Estimation of ionospheric electric fields, ionospheric currents, and field-aligned currents from ground magnetic records. J. Geophys. Res., **86**, 801–813.

KAN, J. R. and BURKE, W. J. (1985): A theoretical model of polar cap auroral arcs. J. Geophys. Res., **90**, 4171–4177.

KILLEEN, T. L. and ROBLE, R. G. (1984): An analysis of the high-latitude thermospheric wind pattern calculated by a thermospheric general circulation model; 1. Momentum forcing. J. Geophys. Res., **89**, 7509–7522.

KILLEEN, T. L., HAYS, P. B., SPENCER, N. W. and WHARTON, L. E. (1982): Neutral winds in the polar thermosphere as measured from Dynamics Explorer. Geophys. Res. Lett., **9**, 957–960.

KILLEEN, T. L., HAYS, P. B., CARIGNAN, G. R., HEELIS, R. A., HANSON, W. B., SPENCER, N. W. and BRACE, L. H. (1984a): Ion-neutral coupling in the high-latitude *F* region: Evaluation of ion heating terms from Dynamics Explorer 2. J. Geophys. Res., **89**, 7495–7508.

KILLEEN, T. L., SMITH, R. W., HAYS, P. B., SPENCER, N. W., WHARTON, L. E. and MCCORMAC, F. G. (1984b): Neutral winds in the high latitude winter *F*-region in coordinated observations from ground and space. Geophys. Res. Lett., **11**, 311–314.

KOKUBUN, S. (1971): Polar substorm and interplanetary magnetic field. Planet. Space Sci., **19**, 697–714.

LASSEN, K. (1969): Polar cap emissions. Atmospheric Emissions, ed. by B. M. MCCORMAC and A. OLMHOLT. New York, Reinhold, 63–71.

LASSEN, K. (1972a): On the classification of high latitude auroras. Geophys. Publ., **29**, 87.

LASSEN, K. (1979): The quiet-time pattern of auroral arcs as a consequence of magnetospheric convection. Danske Meteor. Inst., Copenhagen, R-56.

LASSEN, K. and DANIELSEN, C. (1978): Quiet time pattern of auroral arcs for different directions of interplanetary magnetic field in the *Y-Z* plane. J. Geophys. Res., **83**, 5277–5284.

LYONS, L. R. (1985): A simple model for polar cap convection patterns and generation of θ auroras. J. Geophys. Res., **90**, 1561–1567.

MAEZAWA, K. (1976): Magnetospheric convection induced by the positive and negative Z components of the interplanetary magnetic field; Quantitative analysis using polar cap magnetic records. J. Geophys. Res., **81**, 2289–2303.

MAKITA, K. and MENG, C.-I. (1984): Average electron precipitation patterns and visual aurora characteristics during geomagnetic quiescence. J. Geophys. Res., **89**, 2861–2872.

MAKITA, K., MENG, C.-I. and AKASOFU, S.-I. (1983): The shift of the auroral electron precipitation

boundaries in the dawn-dusk sector in association with geomagnetic activity and interplanetary magnetic field. J. Geophys. Res., **88**, 7967–7981.

MAKITA, K., MENG, C.-I. and AKASOFU, S.-I. (1985): Temporal and spatial variations of the polar cap dimension inferred from the precipitation boundaries. J. Geophys. Res., **90**, 2744–2752.

MAWSON, D. (1925): Records of the aurora polaris. Australas. Antarct. Exped. 1911–1914. Sci. Rep., Ser. B, Vol. 2, Pt. 1, 11.

MCCORMAC, F. G., KILLEEN, T. L., GOMBOSI, E., HAYS, P. B. and SPENCER, N. W. (1985): Configuration of the high-latitude thermosphere neutral circulation for IMF B_y negative and positive. Geophys. Res. Lett., **12**, 155–158.

MCDIARMID, I. B., BURROWS, J. R. and WILSON, M. D. (1980): Comparison of magnetic field perturbations and solar electron profiles in the polar cap. J. Geophys. Res., **85**, 1163–1170.

MENG, C.-I. (1978): Electron precipitations and polar auroras. Space Sci. Rev., **22**, 223–300.

MENG, C.-I. (1981a): Polar cap arcs and the plasma sheet. Geophys. Res. Lett., **8**, 273–276.

MENG, C.-I. (1981b): The auroral electron precipitation during extremely quiet geomagnetic conditions. J. Geophys. Res., **86**, 4607–4627.

MENG, C.-I. and AKASOFU, S.-I. (1976): The relation between the polar cap auroral arc and the auroral oval arc. J. Geophys. Res., **81**, 4004–4006.

MENG, C.-I., AKASOFU, S.-I. and ANDERSON, K. A. (1977): Dawn-dusk gradient of the precipitation of low-energy electrons over the polar cap and its relation to the interplanetary magnetic field. J. Geophys. Res., **82**, 5271–5275.

MERIWETHER, J. W., HEPPNER, J. P., STOLARIK, J. D. and WESCOTT, E. M. (1973): Neutral winds above 200 km at high latitudes. J. Geophys. Res., **78**, 6643–6661.

MISHIN, V. M., BAZARZHAPOV, A. D. and SHPYNEV, G. B. (1980): Electric fields and currents in the earth's magnetosphere. Dynamics of the Magnetosphere, ed. by S.-I. AKASOFU. Dordrecht, D. Reidel, 249–268 (Astrophys. Space Sci. Lib., Vol. 78).

MOZER, F. S. (1984): Electric field evidence on the viscous interaction at the magnetopause. Geophys. Res. Lett., **11**, 135–138.

MURPHREE, J. S., ANGER, C. D. and COGGER, L. L. (1982): The instantaneous relationship between polar cap and oval auroras at times of northward interplanetary magnetic field. Can. J. Phys., **60**, 349–356.

MURPHREE, J. S., ANGER, C. D., MENG, C.-I. and AKASOFU, S.-I. (1984): Largescale auroral distribution and the open field line region. Planet. Space Sci., **32**, 105–109.

NISHIDA, A. (1978): Geomagnetic Diagnosis of the Magnetosphere. New York, Springer, 256 p.

NISHIDA, A. and KAMIDE, Y. (1983): Magnetospheric processes preceding the onset of an isolated substorm; A case study of the March 31, 1978, substorm. J. Geophys. Res., **88**, 7005–7014.

OGINO, T. and WALKER, R. J. (1984): An magnetohydrodynamic simulation of the bifurcation of the tail lobes during intervals with northward interplanetary magnetic field. Geophys. Res. Lett., **11**, 1018–1021.

OGINO, T., WALKER, R. J., ASHOUR-ABDALLA, M. and DAWSON, J. M. (1984): An MHD simulation of B_y-dependent magnetospheric convectional field-aligned current during northward IMF. Plasma Phys. Fusion Eng., UCLA, PPG-805, July. (preprint).

PERREAULT, P. and AKASOFU, S.-I. (1978): A study of geomagnetic storms. Geophys. J. R. Astron. Soc., **54**, 547–573.

PETERSON, W. K. and SHELLEY, E. G. (1984): Origin of the plasma in a crosspolar cap auroral feature (Theta aurora). J. Geophys. Res., **89**, 6729–6736.

POTEMRA, T. A., ZANETTI, L. J., BYTHROW, P. F., LUI, A. T. Y. and IIJIMA, T. (1984): B_y dependent convection patterns during northward interplanetary magnetic field. J. Geophys. Res., **89**, 9753–9760.

REES, D., FULLER-ROWELL, T. J., GORDON, R., KILLEEN, T. L., HAYS, P. B., WHARTON, L. and SPENCER, N. W. (1983): A comparison of wind observations of the upper thermosphere from the Dynamics Explorer satellite with the predictions of a global time-dependent model. Planet. Space Sci., **31**, 1299–1314.

REIFF, P. H. (1984): Evidence of magnetic merging from low-altitude spacecraft and ground-based

experiments. Magnetic Reconnection in Space and Laboratory Plasmas, ed. by E. W. HONES, Jr. Washington, D. C., Am. Geophys. Union, 104–113 (Geophysical Monograph 30).

REIFF, P. H. and BURCH, J. L. (1985): IMF B_y-dependent plasma flow and Birkeland currents in the dayside magnetosphere; 2. A global model for northward and southward IMF. J. Geophys. Res., **90**, 1595–1609.

REIFF, P. H., SPIRO, R. W. and HILL, T. W. (1981): Dependence of polar cap potential drop on interplanetary parameters. J. Geophys. Res., **86**, 7639–7648.

ROBLE, R. G., DICKINSON, R. E. and RIDLEY, E. C. (1982): Global circulation and temperature structure of thermosphere with high-latitude plasma convection. J. Geophys. Res., **87**, 1599–1644.

ROBLE, R. G., EMERY, B. A., DICKINSON, R. E., RIDLEY, E. C., KILLEEN, T. L., HAYS, P. B., CARIGNAN, G. R. and SPENCER, N. W. (1984): Thermospheric circulation, temperature, and compositional structure of the southern hemisphere polar cap during October–November 1981. J. Geophys. Res., **89**, 9057–9068.

ROSTOKER, G. (1980): Magnetospheric and ionospheric currents in the polar cusp and their dependence on the B_y component of the interplanetary magnetic field. J. Geophys. Res., **85**, 4167–4176.

ROSTOKER, G. (1983): Triggering of expansive phase intensifications of magnetospheric substorms by northward turnings of the interplanetary magnetic field. J. Geophys. Res., **88**, 6981–6993.

SAFLEKOS, N. A., POTEMRA, T. A. and IIJIMA, T. (1978): Small-scale transverse magnetic disturbances in the polar regions observed by Triad. J. Geophys. Res., **83**, 1493–1502.

SAFLEKOS, N. A., SHEEHAN, R. E. and CAROVILLANO, R. L. (1982): Global nature of field-aligned currents and their relation to auroral phenomena. Rev. Geophys. Space Phys., **20**, 709–734.

SCHUNK, R. W. and SOJKA, J. J. (1982): Ionospheric hot spot at high latitudes. Geophys. Res. Lett., **9**, 1045–1048.

SIBECK, D. G., SISCOE, G. L., SLAVING, J. A., SMITH, E. J., TSURUTANI, B. T., GOSLING, J. A., LEPPING, R. P. and LAZARUS, A. J. (1985): The distant magnetotail's response to a strong IMF B_z; Twisting, flattening, and flaring. Geophys. Res. Lett. (in press).

SOJKA, J. J. and SCHUNK, R. W. (1983): A theoretical study of the high latitude F region's response to magnetospheric storm inputs. J. Geophys. Res., **88**, 2112–2122.

SOJKA, J. J. and SCHUNK, R. W. (1984): A theoretical F region study of ion compositional and temperature variations in response to magnetospheric storm inputs. J. Geophys. Res., **89**, 2348–2358.

SOJKA, J. J., SCHUNK, R. W., EVANS, J. V., HOLT, J. M. and WAND, R. H. (1983): Comparison of model high-latitude electron densities with Millstone Hill observations. J. Geophys. Res., **88**, 7783–7793.

SVALGAARD, L. (1973): Polar cap magnetic variations and their relationship with the interplanetary magnetic sector structure. J. Geophys. Res., **78**, 2064–2078.

TROSHICHEV, O. A. (1982): Polar magnetic disturbances and field-aligned currents. Space Sci. Rev., **32**, 275–360.

VAMPOLA, A. L. (1971): Access of solar electrons to closed field lines. J. Geophys. Res., **76**, 36–43.

WEBER, E. J., BUCHAU, J., MOORE, J. G., SHARBER, J. R., LIVINGSTON, R. C., WINNINGHAM, J. D. and REINISCH, B. W. (1984): F layer ionization patches in the polar cap. J. Geophys. Res., **89**, 1683–1694.

WINNINGHAM, J. D. and HEIKKILA, W. J. (1974): Polar cap auroral electron fluxes observed with ISIS 1. J. Geophys. Res., **79**, 949–957.

WYGANT, J. R., TORBERT, R. B. and MOZER, F. S. (1983): Comparison of S3-3 polar cap potential drops with the interplanetary magnetic field and models of magnetopause reconnection. J. Geophys. Res., **88**, 5727–5735.

YAU, A. W., WHALEN, B. A., PETERSON, W. K. and SHELLEY, E. G. (1984): Distribution of upflowing ionospheric ions in the high-altitude polar cap and auroral ionosphere. J. Geophys. Res., **89**, 5507–5522.

ZANETTI, L. J., POTEMRA, T. A., IIJIMA, T., BAUMJOHANN, W. and BYTHROW, P. F. (1984): Ionosphere and Birkeland current distributions for northward interplanetary magnetic field; Inferred polar convection. J. Geophys. Res., **89**, 7453–7458.

(Received January 19, 1985; Revised manuscript received October 7, 1985)